Math.Comput.Sci. (2016) 10:179–205
DOI 10.1007/s11786-016-0245-5

Mathematics in Computer Science

Detecting Curves of Symmetry in Images Via Hough Transform

Giorgio Ricca · Mauro C. Beltrametti · Anna Maria Massone

Received: 27 June 2015 / Revised: 10 January 2016 / Accepted: 21 January 2016 / Published online: 1 March 2016

Abstract The Hough transform is a standard pattern recognition technique introduced between the 1960s and the 1970s for the detection of straight lines, circles, and ellipses with several applications including the detection of symmetries in images. Recently, based on algebraic geometry arguments, the procedure has been extended to the automated recognition of special classes of algebraic plane curves. This allows us to detect *curves of symmetry* present in images, that is, curves that recognize midpoints maps of various shapes extracted by an ad hoc symmetry algorithm, here proposed. Further, in the case of straight lines, the detection of lines of symmetry allows us, by a pre-processing step of the image, to improve the efficiency of the recognition algorithm on which the Hough transform technique is founded, without loss of generality and additional computational costs.

Keywords Symmetry detection · Algebraic plane curves · Pattern recognition · Hough transform

Mathematics Subject Classification Primary 68D18 · 68U10; Secondary 14H50 · 92C50

1 Introduction

In pattern recognition domain the Hough transform [9,15] is a well known technique to find shapes in images. In its basic formulation the Hough transform allows one to extract straight lines in an image on the basis of the following easy mathematical principle: choosing points in the equation of a straight line defined in the indeterminates x, y and following the usual slope-intercept parametrization (or the so called normal parametrization) corresponds to draw lines (or sinusoidal curves) in the space of parameters a, b (or θ, ρ) that all intersect in exactly one point. This point uniquely identifies the original straight line in the image space. Analogously, circles and ellipses can be

G. Ricca (✉) · M. C. Beltrametti
Dipartimento di Matematica, Università di Genova, Via Dodecaneso 35, 16146 Genoa, Italy
e-mail: ricca@dima.unige.it

M. C. Beltrametti
e-mail: beltrametti@dima.unige.it

A. M. Massone
CNR-SPIN, Via Dodecaneso 33, 16146 Genoa, Italy
e-mail: annamaria.massone@cnr.it

extracted in an image by searching for a unique intersection point in a 3D or 4D parameter space respectively [9] (see also [17] for more references).

Recently, a formal result based on algebraic geometry arguments has extended the definition of Hough transform to the case of special classes of curves [2,17]. More precisely, a key lemma in [2] (see Lemma 3.3 in the present paper) characterizes those families $\mathcal{F}$ of irreducible algebraic plane curves that share the degree and for which the following general Hough-type correspondence between the image space and the parameter space holds true: each point P of a curve from the family in the image space is transformed into a hypersurface $\Gamma_P(\mathcal{F})$ in the parameter space in such a way that all hypersurfaces $\Gamma_P(\mathcal{F})$ meet in one and only one point uniquely identifying the original curve in the image space. Such families of curves are also called *Hough regular* (see Sect. 3).

From a computational point of view an intrinsic problem of the Hough transform technique consists in the fact that its complexity is exponential with respect to the dimension of the parameter space, i.e. to the number of parameters, which, however, are needed to represent the curves of a given family with due generality.

In this paper, we develop a Hough-type technique able to identify axes of symmetry present in images having in mind a specific application: the knowledge of any symmetry present in the image allows a preliminary roto-translation of the image under investigation, then reducing the number of parameters in the family of curves without loss of generality.

Three types of symmetry can be found in an image: *reflection symmetry* (also called *mirror symmetry* or *line symmetry*), when an axis of symmetry divides an object into halves that are mirror image, *rotation symmetry*, when an object can be turned around its center point to positions in which it looks the same as it does in its original position (note that often rotation symmetry includes reflection symmetry), and *translation symmetry*, when a basic pattern is regularly repeated in a given direction. We are mainly interested in reflection symmetry.

Several methods for detecting symmetries in images have been developed in computer vision and shape analysis, some of them based on the use of the Hough transform. For example, we refer to [16] and [7] for characterizations of symmetries by using the Hough transform for lines detection (the first one uses local feature keypoints, generates mirrored features using arbitrary mirroring axis and then uses the Hough transform to detect symmetric matches, while the second one uses the Hough transform just as initialization step for a more complex algorithm); we refer to [5] for detection of 3D mirror symmetries by using a 3D formulation of the Hough transform for the search of symmetry planes; to [26] for detection of rotational symmetries by using the Hough transform for ellipses. In [27] two methods for detecting skewed and rotational symmetries are presented. In particular, the first method hypothesizes all possible directions for the transverse axis normal to the axis of symmetry. For each possible direction and for each pairs of points in that direction, midpoints are then found and the Hough transform is used to investigate their collinearity. We finally call the attention to the nice survey paper [14] for a wide up to date research literature (132 items) on the Hough transform technique and its applications.

The symmetry algorithm we propose (presented in Sect. 6 of the paper) differs from those used in the above quoted papers. More precisely,

- we make use of standard edge detection algorithms to select points in the image where the intensity rapidly changes (i.e., edge points),
- we define a symmetry criterion involving the direction of the gradient computed at those points,
- we compute the midpoints of the pairs of edge points meeting such a symmetry criterion, and
- we detect the axis of symmetry, via Hough transform, as the line best approximating the midpoints.

Indeed, by using the extended definition of Hough transform [2] recalled above, our technique easily generalizes to the detection of curves of various shapes as *curves of symmetry* in images (see Sect. 6 for explicit examples).

The paper is organized as follows. The first four sections consist of a detailed, unified survey of the Hough technique to detect curves in 2D images. This surveying part also contains significant expository improvements of known results in the literature. Sections 6 and 7 are the innovative part of the paper. More precisely, in the first two sections we survey the mathematical foundations, based on algebraic geometry arguments, on which the Hough transform pattern recognition technique is nowadays founded. Section 2 contains the formal definition and basic set-up of Hough transform with respect to a given family of algebraic plane curves. Special emphasis is given to

the fact that the Hough transform concept generalizes the usual duality of lines and points in projective geometry, leading to a *curves and points duality* notion. Section 3 is focused on special families of curves meeting the Hough regularity property highlighted above, a feature that plays a crucial role in pattern recognition problems. In Sect. 4 we provide several illustrative examples of classes of curves of interest in astronomical and medical imaging. We will recover some of them in Sects. 6 and 7, which are the core of the paper. In Sect. 5 we present the recognition algorithm on which the Hough transform technique is founded. We devoted Sect. 6 to a detailed description and test of the symmetry algorithm we propose. In Sect. 7 we present some applications of the Hough-based symmetry algorithm to medical imaging problems as a pre-processing step for the Hough transform recognition algorithm. In fact, a challenging research topic in medical imaging is the recognition of bone profiles in X-ray Computed Tomography (CT) images, where a priori symmetry analyses of bone structures can be very useful to reduce the number of parameters occurring in the equations of the curves used for recognition purposes. This way one finds a good compromise between generality and computational cost of the recognition algorithm. Finally, our conclusions will be offered in Sect. 8.

2 Hough Transform Via Algebraic Curves

The Hough transform is a standard pattern recognition technique, introduced between the sixties and the seventies, for the detection of straight lines, circles and ellipses. Here we offer a mathematical foundation, based on algebraic-geometry arguments, of an extension of this approach to the automated recognition of special algebraic plane curves of higher degree. We refer to [2,3] and [17] for applications and further developments.

Most of the results in this section hold over an infinite integral ring K (see [11, Section 28]). However, let us restrict to the classical cases where either $K = \mathbb{R}$ or $K = \mathbb{C}$, the fields of real or complex numbers, respectively.

For every t-tuples of independent parameters $\lambda := (\lambda_1, \ldots, \lambda_t)$, varying in an Euclidean open set $\mathcal{U} \subseteq K^t$, and indeterminates x, y, let $\mathcal{P}$ be a family of non-constant irreducible polynomials

$$f_\lambda(x, y) = \sum_{i,j=0}^{d} x^i y^j g_{ij}(\lambda_1, \ldots, \lambda_t), \quad i + j \leq d, \tag{2.1}$$

in $K[x, y]$, of a given degree d (not depending on λ), whose coefficients $g_{ij}(\lambda)$ are the evaluations in the parameters λ of polynomials $g_{ij}(\Lambda) \in K[\Lambda]$ in the variables $\Lambda = (\Lambda_1, \ldots, \Lambda_t)$. Let $\mathcal{F}$ be the corresponding family of the zero loci $\mathcal{C}_\lambda := f_\lambda(x, y) = 0$, and let assume that $\mathcal{C}_\lambda$ is a curve in the affine plane $\mathbb{A}^2_{(x,y)}(K)$, for each λ (of course, this is always the case if $K = \mathbb{C}$). Clearly, if $K = \mathbb{C}$, the curves are irreducible, that is, they consist of a single component, since the polynomials of the family $\mathcal{P}$ are assumed to be irreducible in $K[x, y]$. If $K = \mathbb{R}$, the case of interest in the applications, we assume that $\mathcal{C}_\lambda$ is an *irreducible real affine plane curve*, that is, a curve irreducible over $\mathbb{C}$ with infinitely many points in the affine plane $\mathbb{A}^2_{(x,y)}(\mathbb{R})$ (see also [23, Section 7.1]). Such a real curve may contain a finite set of isolated points; to this purpose, see also Remark 2.4 below. So, we want $\mathcal{F}$ to be a *family of real irreducible curves* (*up to possibly a finite set of points*) *which share the degree*.

We need to take into account, and exclude from our context, obvious exceptions to the above basic assumptions, as the following example shows.

Example 1 Consider the family of real conics

$$\mathcal{C}_{a,b} : x^2 + ay^2 - b = 0,$$

with $\lambda = (a, b) \in \mathbb{R}^2$. Then $\mathcal{C}_{1,0}$ is defined by the polynomial $x^2 + y^2 = 0$ and consists of the single point $(0, 0)$ in $\mathbb{A}^2_{(x,y)}(\mathbb{R})$. While $\mathcal{C}_{-1,0}$ is defined by the polynomial $x^2 - y^2 = 0$ and consists of two distinct lines. Therefore $\mathcal{C}_{1,0}$ is strictly contained in $\mathcal{C}_{-1,0}$. But clearly such a family of conics does not satisfy the basic assumptions made (to be a family of irreducible curves sharing the degree) unless $a \neq 0$ and $b > 0$. Moreover, in the case of the family of conics

$$\mathcal{C}_{a,b} : a^2x^2 + by - 1 = 0,$$

with $a, b \in \mathbb{R}$, note that $\mathcal{C}_{0,0} = \emptyset$, and we need $a \neq 0$ for the degree to be preserved.

Definition 2.1 Let $\mathcal{F}$ be a family of curves $\mathcal{C}_\lambda$ as above, and let $P = (x_P, y_P)$ be a point in the image space $\mathbb{A}^2_{(x,y)}(K)$. Let $\Gamma_P(\mathcal{F})$ be the locus defined in the affine t-dimensional parameter space $\mathbb{A}^t_{(\Lambda_1,\ldots,\Lambda_t)}(K)$ by the polynomial equation

$$f_P(\Lambda) := \sum_{i,j=0}^{d} x_P^i y_P^j g_{ij}(\Lambda_1, \ldots, \Lambda_t) = 0, \quad i + j \leq d, \tag{2.2}$$

in the indeterminates $\Lambda_1, \ldots, \Lambda_t$. We say that $\Gamma_P(\mathcal{F})$ is the *Hough transform of the point P with respect to the family $\mathcal{F}$*. If no confusion will arize, we simply say that $\Gamma_P(\mathcal{F})$ is the *Hough transform of P*.

Remark 2.2 If $K = \mathbb{C}$, or more generally K is algebraically closed, the Hough transform $\Gamma_P(\mathcal{F})$ is a hypersurface in the parameter space.

If $K = \mathbb{R}$, the locus $\Gamma_P(\mathcal{F})$ is a hypersurface if and only if the polynomial $f_P(\Lambda) \in \mathbb{R}[\Lambda_1, \ldots, \Lambda_t]$ has a non-singular zero in $\mathbb{R}^t$ (see [4, Theorem 4.5.1] for details and equivalent conditions). This is in fact the general case since one can show that, for P varying in an Euclidean open set of the image space, $\Gamma_P(\mathcal{F})$ is $(t-1)$-dimensional. Here is an example. Consider the family of conics $\mathcal{C}_\lambda : \lambda_1^2 + \lambda_2^2 + \lambda_3 y^2 = 2x^2 - y^2$, with $\lambda_3 > 0$. Then the Hough transform of the origin O is defined by the equation $\Lambda_1^2 + \Lambda_2^2 = 0$, so that it is the line $\Lambda_1 = \Lambda_2 = 0$ in the parameter space $\langle \Lambda_1, \Lambda_2, \Lambda_3 \rangle$, or even the empty set whenever we assume the parameters λ_1, λ_2 to be positive. While, as soon as the point P varies in the Euclidean open set of the image plane $\mathbb{A}^2_{(x,y)}(\mathbb{R})$ defined by the condition $2x^2 - y^2 > 0$, the Hough transform $\Gamma_P(\mathcal{F})$ is a real quadric in the parameter space.

Indeed, as a special case of a more general result (see [22, Proposition 2.25]), the following fact holds true. *Let $\mathcal{F}$ be a family of curves in $\mathbb{A}^2_{(x,y)}(K)$ as in our setting. Then, for a generic point $P \in \mathbb{A}^2_{(x,y)}(K)$, the Hough transform $\Gamma_P(\mathcal{F})$ is $(t-1)$-dimensional.*

Summarizing, the polynomials family defined by (2.1) gives rise to a polynomial $F(x, y; \Lambda_1, \ldots, \Lambda_t)$ in $K[x, y; \Lambda_1, \ldots, \Lambda_t]$ such that, when evaluated at each point $\lambda = (\lambda_1, \ldots, \lambda_t) \in K^t$ and at each point $P = (x_P, y_P) \in \mathbb{A}^2_{(x,y)}(K)$, gives back the equations

$$\mathcal{C}_\lambda : f_\lambda(x, y) = F(x, y; \lambda_1, \ldots, \lambda_t) = 0 \quad \text{and} \quad \Gamma_P(\mathcal{F}) : F(x_P, y_P; \Lambda_1, \ldots, \Lambda_t) = 0$$

of the curve $\mathcal{C}_\lambda$ and the Hough transform $\Gamma_P(\mathcal{F})$, respectively. And, clearly, the "duality condition" (see also Fig. 1)

$$P \in \mathcal{C}_\lambda \iff f_\lambda(x_P, y_P) = F(x_P, y_P; \lambda_1, \ldots, \lambda_t) = 0 \iff \lambda \in \Gamma_P(\mathcal{F}) \tag{2.3}$$

holds true, allowing us to conclude that

- *the Hough transform $\Gamma_P(\mathcal{F})$ of a point $P = (x_P, y_P)$ of the image plane contains a point $\lambda = (\lambda_1, \ldots, \lambda_t)$ if and only if the curve $\mathcal{C}_\lambda$ from the family passes through P.*

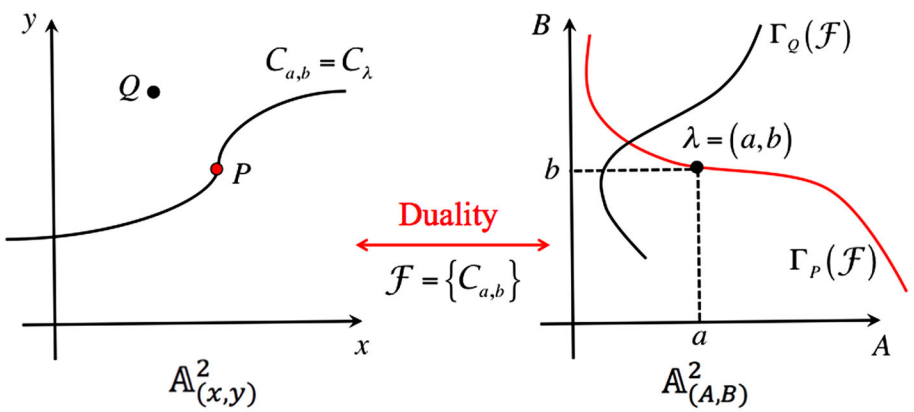

Fig. 1 The Hough transform $\Gamma_P(\mathcal{F})$ of the point P lying on the curve $\mathcal{C}_\lambda$ passes through the point λ in the parameter space, while the Hough transform $\Gamma_Q(\mathcal{F})$, with $Q \notin \mathcal{C}_\lambda$, does not

Let us point out in the following remarks some "patologies" coming out in our context (for instance, actually occurring in Example 6).

Remark 2.3 Notation as above. Of course, it may happen that $\Gamma_P(\mathcal{F}) = \Gamma_Q(\mathcal{F})$ for different points P, Q in the image plane, so that the Hough operator is not injective. Moreover, if P is a *base point* of the family $\mathcal{F} = \{\mathcal{C}_\lambda\}$, that is, all curves $\mathcal{C}_\lambda$ pass through P, the duality condition (2.3) clearly implies $\Gamma_P(\mathcal{F}) = \mathcal{U} \subseteq \mathbb{A}^t_{(\Lambda_1,\dots,\Lambda_t)}(K)$, where $\mathcal{U}$ denotes the variance set of the parameters λ. To this purpose, work to better understand properties of the Hough transform is in progress.

Remark 2.4 (Occurrence of isolated points). Assume $K = \mathbb{R}$, and let $\mathcal{F} = \{\mathcal{C}_\lambda\}$ be a family of real curves as above. Further assume that, for a given $\overline{\lambda} = (\overline{\lambda}_1, \dots, \overline{\lambda}_t)$, the curve $\mathcal{C}_{\overline{\lambda}}$ contains an isolated point, say P. It then follows that P has to be singular of even multiplicity (otherwise the curve would have a real tangent line at P).

We claim that, if the given curve $\mathcal{C}_{\overline{\lambda}}$ contains an isolated point P, then, up to restricting to a suitable Euclidean open subset $\mathcal{U}'$ of the variance set $\mathcal{U} \subseteq \mathbb{A}^t_{(\Lambda_1,\dots,\Lambda_t)}(K)$ of the parameters λ, then P *is an isolated* (*singular*) *point of the general curve* $\mathcal{C}_\lambda$ *from the family, as* λ *varies in* $\mathcal{U}'$. Hence, in particular, P is a base point of the family $\mathcal{F}$ when restricted to $\mathcal{U}'$.

To see this, note that the point P is isolated in a curve $\mathcal{C}_\lambda$ if and only if the minimum

$$d(P, \mathcal{C}_\lambda) := \min\left\{||P - Q||_2 \mid Q \in \mathcal{C}_\lambda \backslash \{P\}\right\}$$

exists and is positive, where $||P - Q||_2$ denotes the usual Euclidean distance, and, moreover, the distance $d(P, \mathcal{C}_\lambda)$ is attained at finite number of m points, for some $m \geq 1$. We refer to [8] for a detailed argument. We can then interpret the set of points $\{\lambda \in \mathbb{R}^t \mid d(P, \mathcal{C}_\lambda) > 0\}$ as

$$\{\lambda \in \mathbb{R}^t \mid d(P, \mathcal{C}_\lambda) > 0\} = d_P^{-1}\big((0, \infty)\big),$$

where the operator $d_P : \mathbb{R}^t \to \mathbb{R}$ is the continuous map defined by $\lambda \mapsto d(P, \mathcal{C}_\lambda)$. Therefore, $\{\lambda \in \mathbb{R}^t \mid d(P, \mathcal{C}_\lambda) > 0\}$ is an open Euclidean set in the parameter space $\mathbb{R}^t$, showing the claimed assertion. Recalling Remark 2.3, we thus conclude that:

(♯) *Up to restricting to an Euclidean open subset* $\mathcal{U}'$ *of the variance open set* $\mathcal{U}$ *of the parameters* λ*, we can always assume that an isolated point* P *of a curve* $\mathcal{C}_\lambda$ *from the family* $\mathcal{F}$ *is a base point of the family, so that the Hough transform* $\Gamma_P(\mathcal{F})$ *coincides with the whole set* $\mathcal{U}'$.

This fact allows us to forget about isolated points when considering intersections of Hough transforms and their properties. We refer to Example 6 for an explicit instance.

3 Hough Regularity

Let $\mathcal{F} = \{\mathcal{C}_\lambda\}$, $\lambda \in \mathcal{U} \subseteq K^t$, be a family of irreducible curves of Eq. (2.1), as in Sect. 2. One main natural question raising from what precedes is:

When the zero loci equality $\mathcal{C}_\lambda = \mathcal{C}_{\lambda'}$ implies $\lambda = \lambda'$?

Remark 3.1 Before to proceed any further, let's pose our attention on what the equality $\mathcal{C}_\lambda = \mathcal{C}_{\lambda'}$ means. If $K = \mathbb{C}$, there is nothing to say. If $K = \mathbb{R}$, we mean that the curves $\mathcal{C}_\lambda, \mathcal{C}_{\lambda'}$ coincide over $\mathbb{C}$ as irreducible real curves, so that they coincide all over their infinitely many real points (a finite set of which may be isolated points). Also, recall that every irreducible real curve has a real defining polynomial (see [23, Lemma 7.2]). Thus, in both cases, $\mathcal{C}_\lambda = \mathcal{C}_{\lambda'}$ expresses as $f_\lambda(x, y) = k f_{\lambda'}(x, y)$ for some non-zero $k \in K$.

This section is devoted to discuss the above question (this way also polishing the proof, in the real case, of [2, Theorem 2.2 and Lemma 2.3] and [17, Lemma 1]). Let us stress the fact that, in the real case, in both Theorem 3.2 and Lemma 3.3 below, when we consider P varying on a curve $\mathcal{C}_\lambda$, and up to restricting the variance set of parameters as in (♯), we may assume P to be not an isolated point. However, such an assumption is not strictly necessary in our setting.

Theorem 3.2 *Consider in $\mathbb{A}^2_{(x,y)}(K)$ a family $\mathcal{F}$ of irreducible curves as above, and let $\mathcal{C}_\lambda$ be a curve of $\mathcal{F}$. Then one has:*

1. *The Hough transforms $\Gamma_P(\mathcal{F})$, when P varies on $\mathcal{C}_\lambda$, all pass through the point $\lambda = (\lambda_1, \ldots, \lambda_t)$.*
2. *Assume that the Hough transforms $\Gamma_P(\mathcal{F})$, when P varies on $\mathcal{C}_\lambda$, have a point in common other than λ, say $\lambda' = (\lambda'_1, \ldots, \lambda'_t)$. Then $\mathcal{C}_\lambda = \mathcal{C}_{\lambda'}$.*

Proof The first statement immediately follows from the duality condition (2.3).

The assumption in the second statement says that $\cap_{P\in\mathcal{C}_\lambda}\Gamma_P(\mathcal{F}) \ni \lambda'$. Then, by using (2.3) again, we conclude that $P \in \mathcal{C}_{\lambda'}$ for each $P \in \mathcal{C}_\lambda$. This implies $\mathcal{C}_\lambda \subseteq \mathcal{C}_{\lambda'}$. If $K = \mathbb{C}$, it follows $\mathcal{C}_\lambda = \mathcal{C}_{\lambda'}$ since $\mathcal{C}_\lambda, \mathcal{C}_{\lambda'}$ are supposed to be irreducible curves of the same degree in the image plane. If $K = \mathbb{R}$, then $\mathcal{C}_\lambda, \mathcal{C}_{\lambda'}$ coincide as real affine plane curves (see Remark 3.1), so we are done. □

The following is an immediate consequence of the above theorem.

Lemma 3.3 (Key Lemma). *Let $\mathcal{F} = \{\mathcal{C}_\lambda\}$ be a family of irreducible curves in $\mathbb{A}^2_{(x,y)}(K)$ as above. Then the following conditions are equivalent.*

1. *For any curves $\mathcal{C}_\lambda, \mathcal{C}_{\lambda'}$ in $\mathcal{F}$, the equality $\mathcal{C}_\lambda = \mathcal{C}_{\lambda'}$ implies $\lambda = \lambda'$;*
2. *For each curve $\mathcal{C}_\lambda$ in $\mathcal{F}$, one has $\cap_{P\in\mathcal{C}_\lambda}\Gamma_P(\mathcal{F}) = \lambda$, where, for $K = \mathbb{R}$, the point P runs all over the real points of the curve $\mathcal{C}_\lambda$.*

Proof Let $K = \mathbb{R}$. Assume (1) to be true. If $\lambda' \in \cap_{P\in\mathcal{C}_\lambda}\Gamma_P(\mathcal{F})$, then Theorem 3.2(2) yields $\mathcal{C}_\lambda = \mathcal{C}_{\lambda'}$, so that $\lambda = \lambda'$ by the present assumption. Thus condition (1) implies condition (2). To show the converse, let $\mathcal{C}_\lambda = \mathcal{C}_{\lambda'}$. Therefore

$$\lambda = \bigcap_{P\in\mathcal{C}_\lambda} \Gamma_P(\mathcal{F}) = \bigcap_{P\in\mathcal{C}_{\lambda'}} \Gamma_P(\mathcal{F}) = \lambda'.$$

If $K = \mathbb{C}$ the same argument works. □

Remark 3.4 The property that a family $\mathcal{F}$ of curves $\mathcal{C}_\lambda$ satisfies the equivalent properties as in Lemma 3.3 expresses as "the Hough transforms $\Gamma_P(\mathcal{F})$ of the points P varying on $\mathcal{C}_\lambda$ intersect in the parameter space in exactly one point which uniquely identifies the curve $\mathcal{C}_\lambda$". Let us stress that this fact plays a crucial role in the pattern recognition problem (see [2, Section 6], [17, Section 4]). In principle, this uniqueness result has just a formal (although elegant) significance, since the presence of more than one point in the parameter space identifying the curve should not prevent the recognition method to properly work. However, in practical applications, the problem of finding such an intersection point becomes a problem of optimization of a matrix (the so called *accumulator*, see Sect. 5 for a detailed description) and the presence of noise on the image pixels often makes the identification of this maximum more ambiguous. Such an ambiguity may be stressed by the presence of more than one maximum in the accumulator.

Clearly, the equivalent properties in Lemma 3.3 are not true in general. For instance, in the case of the family of real conics

$$\mathcal{C}_{a,b} : a^2x^2 + by - 1 = 0,$$

one has $\mathcal{C}_{a,b} = \mathcal{C}_{-a,b}$. Thus, in this case, for the Hough regularity to be true, we need the parameters $\lambda = (a, b)$ vary in a open set $\mathcal{U}$ contained in the half-plane of $\mathbb{R}^2$ defined by $a > 0$ (or $a < 0$).

It is then of special interest to find families of curves which satisfy the equivalent conditions of Lemma 3.3. Indeed, let $\mathcal{C}_\lambda, \mathcal{C}_{\lambda'}$ be curves from the family, and let

$$f_\lambda(x, y) = \sum_{i,j=0}^{d} x^i y^j g_{ij}(\lambda_1, \ldots, \lambda_t), \quad f_{\lambda'}(x, y) = \sum_{i,j=0}^{d} x^i y^j g_{ij}(\lambda'_1, \ldots, \lambda'_t)$$

be the equations of $\mathcal{C}_\lambda$, $\mathcal{C}_{\lambda'}$, respectively. The equality $\mathcal{C}_\lambda = \mathcal{C}_{\lambda'}$ reads $f_\lambda(x, y) = k\, f_{\lambda'}(x, y)$ for some $k \in K^* := K - \{0\}$, that is,

$$\sum_{i,j=0}^{d} x^i y^j \big(g_{ij}(\lambda_1, \ldots, \lambda_t) - k\, g_{ij}(\lambda'_1, \ldots, \lambda'_t)\big)$$

is identically zero on $\mathbb{A}^2_{(x,y)}(K)$ as polynomial in $K[x, y]$. Thus, for each pair of indices i, j, it must be

$$g_{ij}(\lambda_1, \ldots, \lambda_t) = k\, g_{ij}(\lambda'_1, \ldots, \lambda'_t), \quad k \in K^*, \tag{3.1}$$

see [11, Theorem 1, p. 365]. For the classes of curves discussed in Sect. 4 we will use relations (3.1) to show the needed equality $\lambda = \lambda'$.

Let us first recall the well-known cases of lines and circumferences of positive ray (e.g., see [9]) for which the conditions as in Lemma 3.3 clearly hold true.

Example 2 (Lines). Consider in the real projective plane $\mathbb{P}^2_{[x,y,z]}(\mathbb{R})$, where x, y, z are homogeneous coordinates, the family $\mathcal{F}$ of lines $\ell_{u,v,w} : ux + vy + wz = 0$. The space of parameters is now $\mathbb{P}^2_{[U,V,W]}(\mathbb{R})$, where U, V, W are homogeneous coordinates. Let $P = [x_P, y_P, z_P]$ be a point of $\ell_{u,v,w}$. Then the Hough transform $\Gamma_P(\mathcal{F})$ is the line of equation $Ux_P + Vy_P + Wz_P = 0$. Clearly, when P varies on $\ell_{u,v,w}$, such lines belong to the pencil of center $[u, v, w]$, that is, $\cap_{P\in\ell_{u,v,w}}\Gamma_P(\mathcal{F}) = [u, v, w]$.

Note that, in this special case, the notion of Hough transform $\Gamma_P(\mathcal{F})$ of P may be rephrased in terms of the usual duality of the projective plane.

It is just the case to note that the family $\mathcal{F} = \{ux + vy + w = 0\}$ in $\mathbb{A}^2_{(x,y)}(\mathbb{R})$ is not Hough regular, since $\ell_{u,v,w} = \ell_{ku,kv,kw}$ for non-zero constants k. Of course, $\mathcal{F}$ will be Hough regular as soon as one of the parameters u, v, w is a constant.

In practice, passing to affine coordinates, and also to include the lines $x = k$ (not contained, for instance, in the family of lines $\{\ell_{a,b} : y - ax - b = 0\}$), the most convenient representation is the *normal parametrization* of a line ℓ in $\mathbb{A}^2_{(x,y)}(\mathbb{R})$. That is, the equation in polar coordinates ρ, θ of the form

$$\ell : x\cos\theta + y\sin\theta = \rho, \tag{3.2}$$

where θ is the angle from the x-axis to the perpendicular from the origin O to the line, and ρ is the distance of O to the line. By using this expression, the Hough transform is classically studied and its basic properties hold true in this case as well (see [19]). Clearly, letting $\lambda = (\rho, \theta)$, Eq. (3.2) is not of the polynomial form (2.1). Recall that an equation of a line in the general algebraic form

$$\ell : ax + by = c,$$

where a, b, c are real parameters, with $ab \neq 0$ and $c > 0$, can be changed to the normal form by dividing by $\sqrt{a^2 + b^2}$, where

$$\cos\theta = \frac{a}{\sqrt{a^2+b^2}}, \quad \sin\theta = \frac{b}{\sqrt{a^2+b^2}}, \quad \rho = \frac{c}{\sqrt{a^2+b^2}}. \tag{3.3}$$

Example 3 (Circles) In the affine plane $\mathbb{A}^2_{(x,y)}(\mathbb{R})$ consider a family $\mathcal{F}$ of circumferences

$$\gamma_{a,b} : (x - a)^2 + (y - b)^2 = r^2,$$

where the center (a, b) varies and the radius r (> 0) is supposed to be *fixed*. For each given point $P = (x_P, y_P) \in \gamma_{a,b}$, the Hough transform is the circumference $\Gamma_P(\mathcal{F})$ of center (x_P, y_P) and radius r in the parameter plane $\mathbb{A}^2_{(A,B)}(\mathbb{R})$. Clearly one has $\cap_{P\in\gamma_{a,b}}\Gamma_P(\mathcal{F}) = (a, b)$. Note that as r varies, then the Hough transform is a quadric cone of vertex $(a, b, r) = (x_P, y_P, 0)$ in the parameter space $\mathbb{A}^3_{(A,B,R)}(\mathbb{R})$.

We give few more comments to clarify the use of relations (3.1).

Example 4 Consider the one-parameter family of real conics $\mathcal{C}_a = x^2 + a^2 y = 0$. Assuming $\mathcal{C}_a = \mathcal{C}_{a'}$, relations (3.1) become

$$1 = g_{20}(a) = k g_{20}(a') = k, \quad a^2 = g_{01}(a) = k g_{01}(a') = k a'^2,$$

giving $k = 1$ and $a = \pm a'$. Then $a = a'$ as soon as a (a') is assumed to be positive.

Remark 3.5 Consider the three-parameter family of conics

$$\mathcal{C}_\lambda = (\lambda_1 + \lambda_2)x^2 + (\lambda_1 - \lambda_2 + \lambda_3)y + x = 0,$$

where $\lambda_1 \neq -\lambda_2$, $\lambda_1 \neq \lambda_2 - \lambda_3$. Then relations (3.1) give $1 = g_{10}(\lambda) = k g_{10}(\lambda') = k$, and therefore $\lambda_1 + \lambda_2 = \lambda'_1 + \lambda'_2$, $\lambda_1 - \lambda_2 + \lambda_3 = \lambda'_1 - \lambda'_2 + \lambda'_3$. In particular, $\mathcal{C}_{1,1,5} = \mathcal{C}_{3,-1,1}$.

To this purpose, we observe the following useful general fact. Assume that each (non-constant) polynomial $g_{ij}(\lambda_1, \ldots, \lambda_t)$ is linear. Further suppose that for a given pair of indices, say $\bar{i}$, $\bar{j}$, the corresponding coefficient is a constant, e.g., $g_{\bar{i}\,\bar{j}}(\lambda_1, \ldots, \lambda_t) = 1$. Hence relations (3.1) lead to a homogeneous linear system in the t variables $\lambda_1 - \lambda'_1, \ldots, \lambda_t - \lambda'_t$. Moreover, $\mathcal{C}_\lambda = \mathcal{C}_{\lambda'}$ implies $\lambda = \lambda'$ provided that the rank of the matrix associated to the system equals t.

Remark 3.6 It is worth noting that most of all the above formally extends if we consider a family of multivariate degree d polynomials

$$f_\lambda(x_1, \ldots, x_n) = \sum_{i_1, \ldots, i_n} x_1^{i_1} \ldots x_n^{i_n}\, g_{i_1 \ldots i_n}(\lambda_1, \ldots, \lambda_t), \quad i_1 + \cdots + i_n \leq d,$$

defining a family of irreducible hypersurfaces in $\mathbb{A}^n_{\boldsymbol{x}}(K)$ sharing the degree, where $\lambda := (\lambda_1, \ldots, \lambda_t)$ varies in an Euclidean open set $\mathcal{U} \subseteq K^t$, $g_{i_1 \ldots i_n}(\Lambda_1, \ldots, \Lambda_t) \in K[\Lambda_1, \ldots, \Lambda_t]$, and $\boldsymbol{x} := (x_1, \ldots, x_n)$ are affine coordinates. We omit the details since we don't essentially use here such a generalization. We refer for this to [3] and [22], where all the theory has been extended even in the more general case of families of affine varieties defined by a system of polynomial equations.

4 Basic Examples

In this section we discuss few illustrative examples belonging to classes of curves of interest in astronomical and medical imaging, and widely used in recent literature to best approximate bone profiles and typical solar structures such as coronal loops (for instance, see [2,6,17,18,21]). Two of them will be exploited in Sect. 7. These families of curves mainly come from atlas of plane curves as [24], as well as from knowledge of classical tools in algebraic geometry.

Example 5 (Elliptic curve). Consider the family $\mathcal{F} = \{\mathcal{C}_{a,b,m,n}\}$ of unbounded cubic curves of equation

$$\mathcal{C}_{a,b,m,n} : y^2 = m(x - n)^3 - a(x - n) - b, \tag{4.1}$$

for some real parameters $\lambda = (a, b, m, n)$, with $m \neq 0$. Non-singular curves from the family are elliptic curves, that is, of genus one. Equation (4.1) is a slight modification of the so called *Weierstrass form*, and allows us to better pattern after a vertebrae profile (see [20,21] and Example 13).

To show that the family is Hough regular, assume $\mathcal{C}_{a,b,m,n} = \mathcal{C}_{a',b',m',n'}$. Then conditions (3.1) read

$$\begin{aligned}
&an - b - mn^3 = g_{00}(\lambda) = k g_{00}(\lambda') = k(a'n' - b' - mn^3),\\
&-1 = g_{02}(\lambda) = k g_{02}(\lambda') = -k,\\
&m = g_{30}(\lambda) = k g_{30}(\lambda') = km'\\
&-3mn = g_{20}(\lambda) = k g_{20}(\lambda') = -3km'n'\\
&3n^2 m - a = g_{10}(\lambda) = k g_{10}(\lambda') = k(3n'^2 m' - a').
\end{aligned}$$

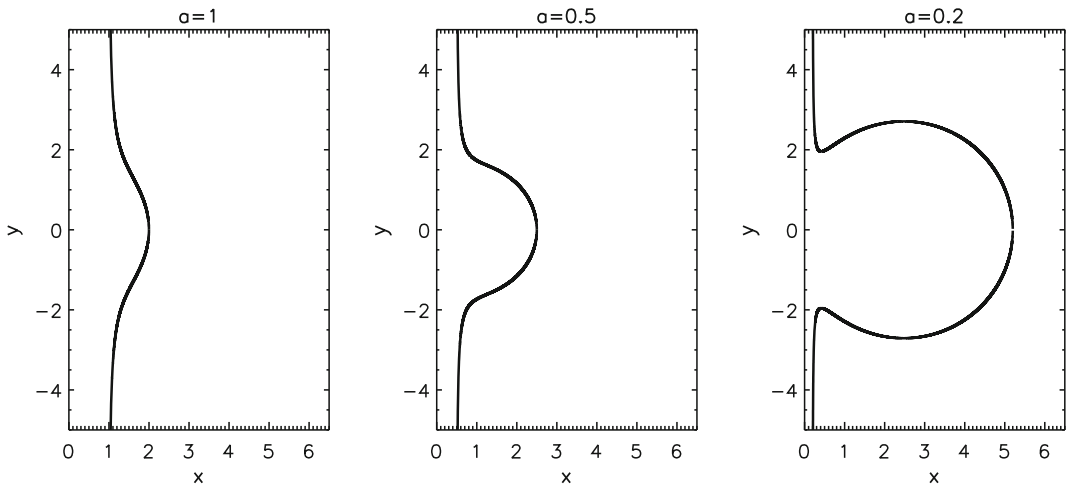

Fig. 2 Shapes of conchoid of Slüse with parameter value $b = 1$

The second, third and fourth relations clearly give $m = m'$ and $n = n'$. Then $a = a'$ by the last relation. Thus the first one yields $b = b'$.

For any point $P = (x_P, y_P)$ in the image plane $\mathbb{A}^2_{(x,y)}(\mathbb{R})$, the Hough transform of P with respect to $\mathcal{F}$ is the quartic hypersurface in the parameter space $\mathbb{A}^4_{(A,B,M,N)}(\mathbb{R})$ of equation

$$\Gamma_P(\mathcal{F}) : M(x_P - N)^3 - A(x_P - N) - B - y_P^2 = 0.$$

Example 6 (Conchoid of Slüse). In the affine plane $\mathbb{A}^2_{(x,y)}(\mathbb{R})$ consider the family $\mathcal{F} = \{\mathcal{C}_{a,b}\}$ of rational cubic curves defined by the equation

$$\mathcal{C}_{a,b} : a(x - a)(x^2 + y^2) = b^2x^2, \tag{4.2}$$

for some positive real numbers a, b. Such a cubic is classically known as *conchoid of Slüse* of parameters a, b (see Fig. 2).

The curve has a double nodal point at the origin O, with complex conjugate tangent lines of equation $a^2(x^2 + y^2) + b^2x^2 = 0$, so that O is an isolated point of the curve. By intersecting with the pencil of lines $y = tx$, we find the parametric rational representation

$$\mathcal{C}_{a,b} : \begin{cases} x = a + \dfrac{b^2}{a(1+t^2)} \\ y = \left(a + \dfrac{b^2}{a(1+t^2)}\right) t \end{cases}$$

For any point $P = (x_P, y_P)$ in the image space $\mathbb{A}^2_{(x,y)}(\mathbb{R})$, the Hough transform is an ellipse in the parameter plane $\mathbb{A}^2_{(A,B)}(\mathbb{R})$ of equation

$$\Gamma_P(\mathcal{F}) : (x_P^2 + y_P^2)A^2 + x_P^2B^2 - x_P(x_P^2 + y_P^2)A = 0.$$

Assume now $\mathcal{C}_{a,b} = \mathcal{C}_{a',b'}$. Relations (3.1) give

$$-a = g_{30}(a, b) = kg_{30}(a', b') = -ka'$$
$$a^2 = g_{02}(a, b) = kg_{02}(a', b') = ka'^2$$
$$a^2 + b^2 = g_{20}(a, b) = kg_{20}(a', b') = k(a'^2 + b'^2)$$

for some $k \in \mathbb{R}^*$. From the two first relations we infer that $k^2 = k$, whence $k = 1$, and therefore $a = a'$. Then the third relation yields $b^2 = b'^2$, so that $b = b'$ since b, b' are positive. Thus the conditions of Lemma 3.3 hold true.

Example 7 (Curve with m convexities). The *curve with m convexities* is defined by the polar equation

$$\mathcal{C}_{a,b,m} : \rho = \frac{a}{1 + b\cos(m\theta)}, \tag{4.3}$$

where a, b are real positive numbers such that $b < 1$, and $m \geq 2$ is an integer.

Such a curve is bounded. In fact, computing the derivative with respect to θ in Eq. (4.3) we find

$$\rho' = \frac{abm\sin(m\theta)}{(1 + b\cos(m\theta))^2}.$$

Therefore $\rho' = 0$ if and only if $\theta = \frac{k}{m}\pi$ for some integer k. For such values of θ, Eq. (4.3) gives

$$\rho_{\min} := \frac{a}{1+b}, \quad \rho_{\max} := \frac{a}{1-b}$$

according to whether k is even or odd, respectively. Thus, the graph of the curve is contained in the circular crown of radii $\frac{a}{1+b}$, $\frac{a}{1-b}$.

The case $m = 3$ looks of interest in some application to medical imaging (see [17,18] and Example 11). In this case, the curve has degree 6 and a direct computation yields the cartesian equation

$$\mathcal{C}_{a,b} : (x^2 + y^2)^3 = \left(a(x^2 + y^2) - b(x^3 - 3xy^2)\right)^2. \tag{4.4}$$

A direct numerical check shows that the origin $O = (0, 0)$ is the only singular point, of multiplicity 4, of the curve $\mathcal{C}_{a,b}$. The tangent cone at O is made up of two complex and conjugate lines, each one counted twice, of total equation

$$(x^2 + y^2)^2 = 0.$$

In particular, over the reals, O is an isolated point. Letting $\ell_1 : x + iy = 0$, $\ell_2 : x - iy = 0$ be the two distinct tangent lines at O, one sees that the intersection multiplicity $m_O(\mathcal{C}_{a,b}, \ell_j)$ of $\mathcal{C}_{a,b}$ with ℓ_j, $j = 1, 2$, equals six (one unity bigger than the general case). We say in this case that O is a *biflecnode* (see e.g. [1, Sections 4.2 and 9.2.5]). In fact, such a singularity forces the curve to be rational. By using Maple 16 `algcurves` package, we find for the curve with 3 convexities $\mathcal{C}_{a,b}$ a (rather complicate) rational parametric expression. For instance, in the case $a = b = 1$, it becomes

$$\mathcal{C}_{1,1} : \begin{cases} x = \dfrac{-t^6 - t^4 + t^2 + 1}{18t^4 - 12t^2 + 2} \\ y = \dfrac{t^5 + 2t^3 + t}{9t^4 - 6t^2 + 1} \end{cases}$$

Moreover, for each $m \geq 2$, the curve is symmetric with respect to the origin and to the m lines of equations

$$x\sin\left(\frac{k\pi}{m}\right) - y\cos\left(\frac{k\pi}{m}\right) = 0, \qquad k = 0, 1, \ldots, m-1.$$

The shape of the curve with 3 convexities strongly depends on the values of the parameters. In particular, a is a sort of scale factor, while, as much as the value of b increases as much the convexities of the curve are sharpened. Figure 3 shows the curve for three different values of b with a fixed to 1.

As far as the Hough transform is concerned, fix a point $P = (x_P, y_P)$ in the image space $\mathbb{A}^2_{(x,y)}(\mathbb{R})$. Then the Hough transform of P with respect to the family $\mathcal{F} = \{\mathcal{C}_{a,b}\}$ is a degenerate conic $\Gamma_P(\mathcal{F}) : r_- \cup r_+$ in the parameter plane $\mathbb{A}^2_{(A,B)}(\mathbb{R})$, i.e., the union of the parallel lines

$$r_\mp : A(x_P^2 + y_P^2) - B(x_P^3 - 3x_P y_P^2) \mp \sqrt{(x_P^2 + y_P^2)^3} = 0.$$

The fact that $\Gamma_P(\mathcal{F})$ is a degenerate conic could make the maximization of the accumulator function particularly challenging. It is then worth noting that the line

$$r_+ : A(x_P^2 + y_P^2) - B(x_P^3 - 3x_P y_P^2) + \sqrt{(x_P^2 + y_P^2)^3} = 0$$

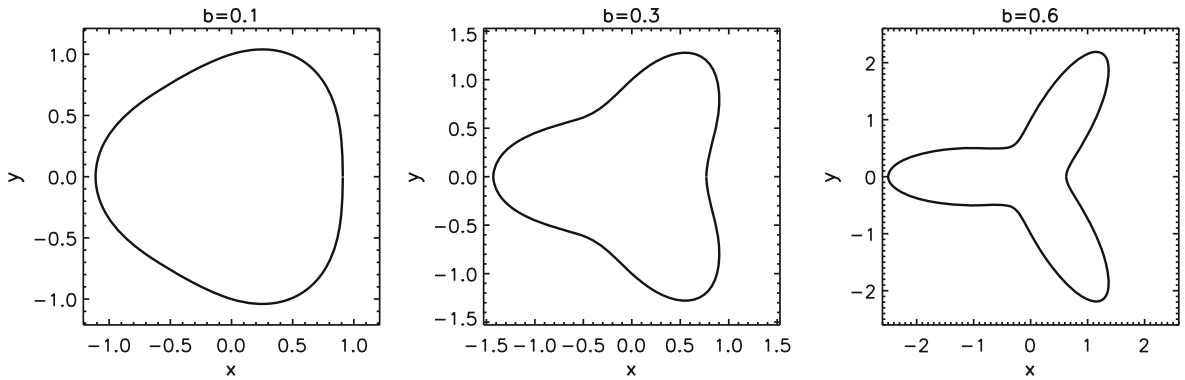

Fig. 3 Three curves with 3 convexities with $a = 1$ and, from *left* to *right*, $b = 0.1$, $b = 0.3$, and $b = 0.6$

doesn't cross the region of interest to be discretized, defined by the conditions $a > 0$, $1 > b > 0$ (see [18, Paragraph 2.1]). Therefore, in practice, the Hough transform of P can be assumed to be the single line of equation

$$r_- : A(x_P^2 + y_P^2) - B(x_P^3 - 3x_P y_P^2) - \sqrt{(x_P^2 + y_P^2)^3} = 0.$$

The usual numerical check, by using conditions (3.1), shows that the family $\mathcal{F}$ is Hough regular.

Example 8 (Curve of Lamet). Consider the family $\mathcal{F} = \{\mathcal{C}_{a,b}\}$ of curves of degree m of equation $\frac{x^m}{a^m} + \frac{y^m}{b} = 1$ or, in polynomial form (2.1),

$$\mathcal{C}_{a,b} : bx^m + a^m y^m = a^m b, \tag{4.5}$$

for positive real numbers a, b. Clearly, the curve $\mathcal{C}_{a,b}$ is non-singular. By using standard facts about p-norms in $\mathbb{R}^n$ (e.g., see [12]), we easily study the variance of the curve of Lamet, which is bounded for even values of m. Note that, for instance, the case $m = 3$ leads to the unbounded Fermat cubic curve. Indeed, consider the diagonal matrix

$$W = \begin{pmatrix} \frac{1}{a} & 0 \\ 0 & \sqrt[m]{\frac{1}{b}} \end{pmatrix},$$

and compute the norm of the matrix product $W\mathbf{v}$, where $\mathbf{v}$ is the column vector $\begin{pmatrix} x_P \\ y_P \end{pmatrix}$. Since $a, b > 0$ and m is even, we find

$$||W\mathbf{v}||_m := \sqrt[m]{\frac{|x_P|^m}{a^m} + \frac{|y_P|^m}{b}} = \sqrt[m]{\frac{x_P^m}{a^m} + \frac{y_P^m}{b}},$$

where $P = (x_P, y_P)$ is a point in the image plane. Thus, $P \in \mathcal{C}_{a,b}$ if and only if $||W\mathbf{v}||_m = 1$. Since

$$||W\mathbf{v}||_\infty := \max\left\{\frac{|x_P|}{a}, \frac{|y_P|}{\sqrt[m]{b}}\right\} \leq ||W\mathbf{v}||_m$$

for $m \geq 1$, one then has $\max\left\{\frac{|x_P|}{a}, \frac{|y_P|}{\sqrt[m]{b}}\right\} \leq 1$. In conclusion, the curve of Lamet is contained in the rectangular region

$$\left\{P = (x_P, y_P) \in \mathbb{A}^2_{(x,y)}(\mathbb{R}) \;\middle|\; -a \leq x_P \leq a,\ -b^{1/m} \leq y_P \leq b^{1/m}\right\}.$$

For each point $P = (x_P, y_P)$ in the image plane, the Hough transform is the $(m+1)$-degree curve in the parameter plane $\mathbb{A}^2_{(A,B)}(\mathbb{R})$ of equation

$$\Gamma_P(\mathcal{F}) : Bx_P^m + A^m y_P^m = A^m B.$$

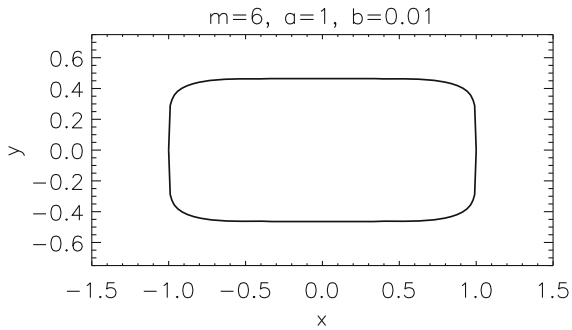

Fig. 4 Curve of Lamet with $m = 6$ and $a = 1$, $b = 0.01$

The curve $\Gamma_P(\mathcal{F})$ has a singular point at the infinity; indeed [0, 1, 0] is a point of multiplicity m, showing that $\Gamma_P(\mathcal{F})$ is a rational curve. A simple rational parametric representation is given by

$$\Gamma_P(\mathcal{F}) = \begin{cases} A = u \\ B = \dfrac{u^m y_P^m}{u^m - x_P^m} \end{cases}, \quad u \in \mathbb{R}.$$

Finally, assume $\mathcal{C}_{a,b} = \mathcal{C}_{a',b'}$. Regularity conditions (3.1) rewrite in this case $g_{ij}(\lambda) = k g_{ij}(\lambda')$, $(i, j) = (m, 0), (0, m), (0, 0)$, leading to

$$b = kb', \quad a^m = ka'^m, \quad -a^m b = -ka'^m b'$$

for some $k \in \mathbb{R}\backslash\{0\}$, respectively. Then $ka'^m b' = a^m b = k^2 a'^m b'$, so that $k^2 = k$, whence $k = 1$. Therefore $b = b'$ and $a^m = a'^m$; since $a > 0$ it follows $a = a'$. Thus, the family $\mathcal{F}$ is Hough regular.

In Fig. 4 we show the graph of a curve of Lamet.

5 The Recognition Algorithm

The technique which implements the Hough transform method is based on a suitable discretization of the parameter space. We briefly describe here the algorithm on which such a technique is founded. Let $\mathcal{F} = \{\mathcal{C}_\lambda\}$ be a family of curves satisfying one of the two equivalent regularity conditions as in Lemma 3.3. From now on, throughout the paper, we will assume $K = \mathbb{R}$.

1. Consider a discretization in a region $\mathcal{T}$ of the parameter space $\mathbb{A}^t_{(\Lambda_1,\dots,\Lambda_t)}(\mathbb{R})$, as follows. First, choose an *initializing point* $\lambda^* = (\lambda_1^*, \dots, \lambda_t^*)$ in $\mathcal{T}$ and let d_k be the *sampling distance with respect to the component* λ_k. Then set

$$\lambda_{k,n_k} := \lambda_k^* + n_k d_k, \quad k = 1, \dots, t, \quad n_k = 0, \dots, N_k - 1, \tag{5.1}$$

where $N_k \in \mathbb{N}$ denotes the number of considered samples for each component, and n_k the index of the sample. Then denote by

$$\mathbf{C}(\mathbf{n}) := \left\{ \lambda = (\lambda_1, \dots, \lambda_t) \in \mathcal{T} \;\middle|\; \lambda_k \in \left[\lambda_{k,n_k} - \frac{d_k}{2}, \lambda_{k,n_k} + \frac{d_k}{2}\right),\ k = 1, \dots, t \right\} \tag{5.2}$$

the cell with center in the *sampling point* $\lambda_{\mathbf{n}} := (\lambda_{1,n_1}, \dots, \lambda_{t,n_t})$ of the parameterized region $\mathcal{T}$, where $\mathbf{n}$ denotes the multi-index $(n_1, \dots, n_t)$. We refer to $\mathbf{C}(\mathbf{n})$ as *the cell represented by the point* $\lambda_{\mathbf{n}}$, and we also denote by $\mathbf{C}(\lambda)$ the cell containing the point $\lambda \in \mathcal{T}$.

Let us stress the fact that the discretization is defined by relation (5.1), that is, by the choice of the initializing point $\lambda^* \in \mathcal{T}$ and the *discretization step* $d := (d_1, \ldots, d_t)$. We will also denote a discretization by $\{\lambda^*, d\}$.

2. We define a multi-matrix $H = (h_{n_1 n_2 \ldots n_t})$ of type $N_1 \times \cdots \times N_t$, called the *accumulator matrix*, or *accumulator function*. One first initializes each entry $H(\mathbf{n}) := h_{n_1 n_2 \ldots n_t}$ of H by setting

$$H(\mathbf{n}) = 0, \quad n_k = 0, \ldots, N_k - 1, \quad k = 1, \ldots, t.$$

3. Choose a number of points of interest, say P_j, $j = 1, \ldots, \nu$, in the image space $\mathbb{A}^2_{(x,y)}(\mathbb{R})$. Consider in $\mathbb{A}^t_{(\Lambda_1,\ldots,\Lambda_t)}(\mathbb{R})$ the Hough transform $\Gamma_{P_j}(\mathcal{F})$ of the point $P_j =: \boldsymbol{x}_j$ of Eq. (2.2), that is,

$$\Gamma_{P_j}(\mathcal{F}) = \left\{\lambda \in \mathbb{A}^t_{(\Lambda_1,\ldots,\Lambda_t)}(\mathbb{R}) \mid F(\boldsymbol{x}_j, \lambda) = 0\right\}, \ j = 1, \ldots, \nu.$$

Then define

$$H(\mathbf{n}) := h_{n_1 n_2 \ldots n_t} := \#\{P_j \mid \Gamma_{P_j}(\mathcal{F}) \cap \mathbf{C}(\mathbf{n}) \neq \emptyset, \ 1 \leq j \leq \nu\}.$$

That is, $H(\mathbf{n})$ is the number of the points P_j such that the corresponding Hough transform $\Gamma_{P_j}(\mathcal{F})$ passes through the cell $\mathbf{C}(\mathbf{n})$, $1 \leq j \leq \nu$. We also refer to this step as to the process of *voting the accumulator matrix*. See Example 9 for the discussion of a special notable case.

Let us point out a parallelism between the exact context discussed in Sect. 2 and the present discretized setting. Indeed, duality relation (2.3) can be interpreted as saying that the above condition $\Gamma_{P_j}(\mathcal{F}) \cap \mathbf{C}(\mathbf{n}) \neq \emptyset$ assures $\mathcal{C}_{\lambda_\mathbf{n}}$ to be a curve approximating the points P_j's. That is, when the discretization step d tends to zero the inequality $\Gamma_{P_j}(\mathcal{F}) \cap \mathbf{C}(\mathbf{n}) \neq \emptyset$ becomes a passage condition through the center $\lambda_\mathbf{n}$ of the cell $\mathbf{C}(\mathbf{n})$. In symbols, for $j = 1, \ldots, \nu$,

$$\lim_{d \to 0} \left(\Gamma_{P_j}(\mathcal{F}) \cap \mathbf{C}(\mathbf{n}) \neq \emptyset\right) = \lambda_\mathbf{n} \in \Gamma_{P_j}(\mathcal{F}).$$

4. We want to find a curve from the family $\mathcal{F}$, say $\mathcal{C}_{\lambda^{\text{opt}}}$, best approximating the profile of interest (which determines, of course, the choice of the data set of points P_j's as in Step 3, some of them possibly perturbed by noise). Let $\lambda^{\text{opt}} = (\lambda_1^{\text{opt}}, \ldots, \lambda_t^{\text{opt}})$ be the center of the cell $\mathbf{C}(\mathbf{n})$ whose corresponding entry $h_{n_1 n_2 \ldots n_t}$ of the accumulator matrix will take (local) maximum value m.[1] By what previously observed, the curve $\mathcal{C}_{\lambda^{\text{opt}}}$ approximates the maximum number, m, of points among $P_1, \ldots, P_\nu$. This suggests $\mathcal{C}_{\lambda^{\text{opt}}}$ as a potential candidate curve to best approximate the profile of interest.

Note that Theorem 3.2 and Lemma 3.3 establish a theoretical support to overcome a possible ambiguity due to the presence of noise in the image. More precisely, assume that the previous argument leads to a further cell $\mathbf{C}(\mathbf{n}')$, corresponding to the entry $h_{n'_1 n'_2 \ldots n'_t}$ of the accumulator matrix H, giving a "false" (local) maximum m due to the presence of noise among the points P_j's. In such a way, we would find a further potential candidate curve $\mathcal{C}_{\lambda^{\text{opt}'}}$ to approximate the profile. Thus, Theorem 3.2(2) suggests the identity $\mathcal{C}_{\lambda^{\text{opt}}} = \mathcal{C}_{\lambda^{\text{opt}'}}$ to be true. In an exact context, the regularity property then would apply to give $\lambda^{\text{opt}} = \lambda^{\text{opt}'}$, so that the curve $\mathcal{C}_{\lambda^{\text{opt}}}$ would be univocally determined by the parameter λ^{opt}.

Of course, λ^{opt} is determined up to the discretization $\{\lambda^*, d\}$.

5. To explicitly find the cell $\mathbf{C}(\mathbf{n})$ represented by the point λ^{opt}, make a scanning of the accumulator function. By computing its maximum we then determine the t-tuple $(\lambda_1^{\text{opt}}, \ldots, \lambda_t^{\text{opt}})$ which represents the cell in question and which characterizes the equation of the seeked curve $\mathcal{C}_{\lambda^{\text{opt}}}$ best recognizing the profile of interest.

Figure 5 describes the behavior of the recognition algorithm for an elliptic curve of Eq. (4.1), where in the recognition procedure we take as known the parameters n and b and we try to recover the parameters m and a. We

[1] Note that if two or more local maxima are obtained in different cells, they essentially correspond to two or more different curves from the family.

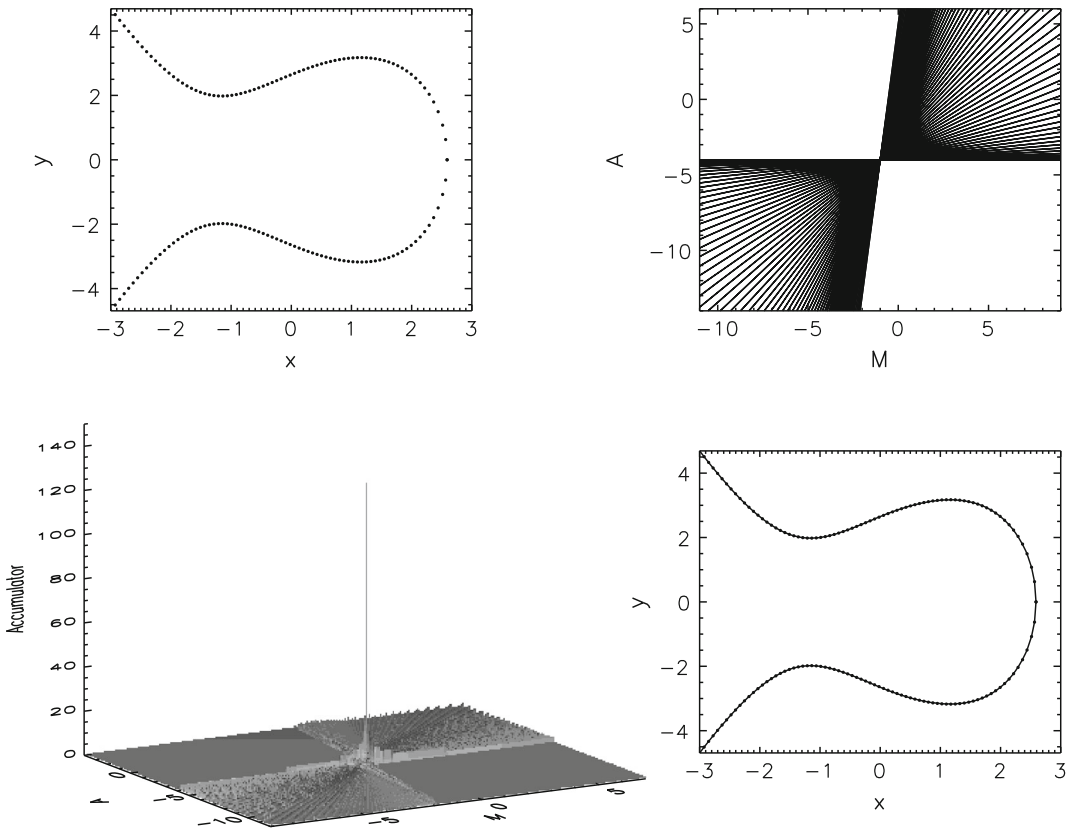

Fig. 5 Recognition of an elliptic curve, Eq. (4.1) with $m = -1$, $n = 0$, $a = -4$ and $b = -7$. *Top left* dataset points sampled on the curve; *top right* Hough transforms of the dataset points; *bottom left* accumulator function; *bottom right* recognized curve with dataset points superimposed

start from a synthetic dataset of 154 points satisfying the curve equation (Fig. 5, top left panel) and we show the Hough transforms of the points in the dataset (straight lines in the parameter space $\mathbb{A}^2_{(M,A)}(\mathbb{R})$, Fig. 5, top right panel), the accumulator function (Fig. 5, bottom left panel), and the result of the recognition (Fig. 5, bottom right panel).

Example 9 (Voting the accumulator matrix in the case of rational Hough transforms). In "most cases", for $t = 2$ parameters, the Hough transform turns out to be a rational plane curve. For instance, this is always the case when the polynomials $g_{ij}(\lambda)$ occurring in Eq. (2.1) are either linear or quadratic in the parameters $\lambda = (a, b)$, so that the Hough transforms are either lines or conics (see [2,17] for explicit examples).

With the notation as above, let's assume that, for a general point P in the image plane $\mathbb{A}^2_{(x,y)}(\mathbb{R})$, the Hough transform $\Gamma_P(\mathcal{F})$ is a rational curve in the parameter plane $\langle A, B\rangle$. It can be therefore expressed in the parametric form (compare with Example 8):

$$\Gamma_P(\mathcal{F}) = \begin{cases} A = \dfrac{a_1(u)}{b_1(u)} \\ \\ B = \dfrac{a_2(u)}{b_2(u)} \end{cases}, \quad u \in \mathbb{R},$$

where $a_1(u), a_2(u), b_1(u), b_2(u)$ are polynomials in $\mathbb{R}[u]$. Thus the condition

$\Gamma_P(\mathcal{F}) \cap \mathbf{C}(\mathbf{n}) \neq \emptyset$

as in Step 3) above is equivalent to ask that the system of polynomials inequalities

$$\left(\lambda_{1,n_1} - \frac{d_1}{2}\right) b_1(u) \leq a_1(u) < \left(\lambda_{1,n_1} + \frac{d_1}{2}\right) b_1(u)$$
$$\left(\lambda_{2,n_2} - \frac{d_2}{2}\right) b_2(u) \leq a_2(u) < \left(\lambda_{2,n_2} + \frac{d_2}{2}\right) b_2(u)$$

has a solution.

Remark 5.1 (Presence of "false" maxima). Le $\mathcal{F}$ be a family of curves $\mathcal{C}_\lambda : f_\lambda(x, y) = 0$ as in Sect. 2. Assume that the defining polynomial $f_\lambda(x, y)$ is identically zero for $\lambda = (0, 0, \ldots, 0) =: \mathbf{0}$, that is, the locus $\mathcal{C}_\mathbf{0}$ is the whole image plane $\mathbb{A}^2_{(x,y)}(\mathbb{R})$. By the duality condition (2.3), we then have in the parameter space:

$(0, 0, \ldots, 0) \in \Gamma_P(\mathcal{F})$ for each point $P \in \mathbb{A}^2_{(x,y)}(\mathbb{R})$.

The fact that *all* Hough transform pass through the origin of the parameter space clearly leads to a "false" maximum when we discretize a region $\mathcal{T}$ containing the origin. Even if we assume $\lambda \neq (0, 0, \ldots, 0)$ when defining the family $\mathcal{F} = \{\mathcal{C}_\lambda\}$, this situation may cause serious problems in the determination of the maximum of the accumulator function as in Step 5 of the recognition algorithm outlined above, mainly depending on the shape of the Hough transforms. An accurate case by case ad hoc argument may be needed to overcome the problem.

Relevant cases where this problem actually occurs are the conchoid of Slüse and the Lamet curve described in Examples 6 and 8, respectively.

Remark 5.2 The computation of the accumulator function and its maximization is the most time-consuming step of the algorithm. Further, it strongly depends on the number of parameters, since the dimension of the domain of this function is given by the number of parameters in the game. Even though the theory, and the algorithmic aspects, presented in this section hold true in the above general framework, in practice, the computational burden associated to the accumulator function computation and optimization leads to the need of restricting to families of curves depending on a small number of parameters.

On the other hand, evidences show how including roto-translations and even scaling of the variables is a matter of importance (see, for instance, the discussion in [6, Remark 2.1 and Paragraph 3.1]), this increasing (by up to six) the number t of the parameters $\lambda = (\lambda_1, \ldots, \lambda_t)$ and then making heavier all computations. Work to establish such a relevant extent is in progress (we also refer to [25] for related results). The symmetry algorithm and its applications, presented in Sects. 6 and 7 below, offer a new, alternative, valuable approach to characterize reflection symmetries and then to decrease the dimension of the parameter space.

6 The Symmetry Algorithm

A *continuous image* may be defined as a 2-dimensional continuous function, with respect to the Euclidean topology,

$f : R_1 \times R_2 \to [0, \infty) \subset \mathbb{R}$,

where R_1, R_2 are closed Euclidean intervals in $\mathbb{R}$, x and y are plane coordinates, and the value (also called *amplitude*) of f at any pair of coordinates (x, y) is called the *intensity* of the image at that point. When x, y and the amplitude values of f are all finite, discrete quantities, we call the image a *digital image* and we refer to the intensity values as *gray levels*. Note that a digital image is composed by a finite number of elements, each of which has a particular location and value. These elements are referred to as *pixels*.

To convert the continuous image represented by the function f to digital form, we have to sample the function in both coordinates (*sampling*) and in amplitude (*quantization*). The function $f = f(x, y)$ is then a *digital image*

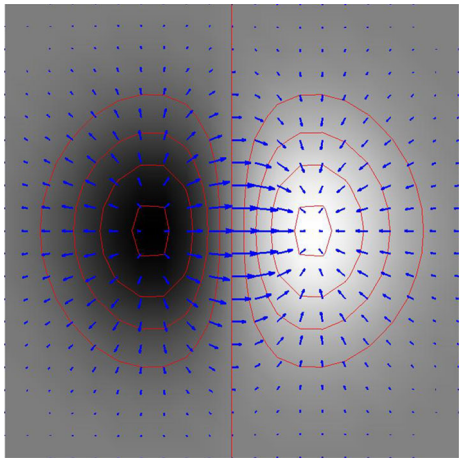

Fig. 6 Sample image in *gray* levels where *black* and *white* colors represent the minimum and maximum value respectively, isolines of the image intensity (*red contours*), and gradient field of the image (*blue arrows*)

if $(x, y) \in \mathbb{Z}_+^2$ and f is a function that assigns a gray level value (that is a real number) to each distinct pair of coordinates (x, y). The result of sampling and quantization is a matrix $f = \{f_{i,j}\}$ whose entries are real numbers (see [13] for basic concepts and methodologies for digital image processing).

The algorithm for the search of axes of symmetry in images is based on a fundamental ingredient, the computation of the numerical gradient of the image, and on the assumption that pairs of points where gradient directions are similar can not be symmetrical with respect to an axis of symmetry.

Given a digital image $f = \{f_{i,j}\}$, where $i = 1, \ldots, I$ and $j = 1, \ldots, J$, the image gradient outlines directional changes in the gray levels of the image. At each image point (i.e., at each pixel), the gradient points in the direction of largest possible intensity increase, and its magnitude corresponds to the rate of change in that direction (see Fig. 6). As a consequence, in image processing, the gradient is commonly used to detect boundaries of objects present in images (i.e., for *edge detection* purposes). As for the computation of the gradient is concerned, recall that an image is a matrix whose entries are determined by particular locations and values. Then, to compute the gradient, just approximations of the derivatives in the horizontal and vertical directions can be defined. The most common way to compute them is to convolve the input image with a kernel (see [13, Chapter 3, Section 3.7.3] for a basic description on computation and use of the gradient in digital image processing).

The symmetry algorithm is made of the following steps.

1. *Computation of the gradient.* Gradient images $f^{(x)}$ and $f^{(y)}$, in the x and y directions respectively, are computed by using Sobel's gradient operator ([13], p. 136). The Sobel operator uses two 3×3 kernels $S^{(x)} = \left\{S_{m,n}^{(x)}\right\}$ and $S^{(y)} = \left\{S_{m,n}^{(y)}\right\}$, $m, n = -1, 0, 1$, where

$$S^{(x)} = \begin{bmatrix} -1 & 0 & 1 \\ -2 & 0 & 2 \\ -1 & 0 & 1 \end{bmatrix} \qquad S^{(y)} = \begin{bmatrix} -1 & -2 & -1 \\ 0 & 0 & 0 \\ 1 & 2 & 1 \end{bmatrix}, \tag{6.1}$$

which are convolved with the original image to calculate numerical approximations of the derivatives, that is,

$$f_{i,j}^{(x)} = \sum_{m=-1}^{1} \sum_{n=-1}^{1} S_{m,n}^{(x)} f_{i+m,j+n} \quad \text{and} \quad f_{i,j}^{(y)} = \sum_{m=-1}^{1} \sum_{n=-1}^{1} S_{m,n}^{(y)} f_{i+m,j+n}. \tag{6.2}$$

The set $\mathcal{S}$ of pixels where the gradient magnitude is greater than a fixed threshold defines the set of edge points.

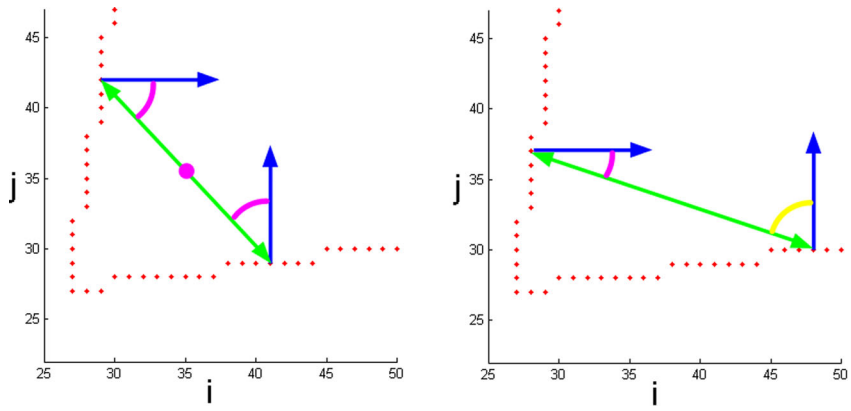

Fig. 7 Symmetry condition applied to two different pairs of edge points (*red dots*). *Left* the selected pair of points satisfies the symmetry condition and then the corresponding middle point (*purple dot*) is added to the midpoint map. *Right* the symmetry condition is not satisfied (angles outlined by *purple* and *yellow arcs* are clearly different), so the considered pair of points does not contribute to the midpoint map

2. *Computation of the gradient direction.* The gradient direction in each pixel $P = (i, j) \in \mathcal{S}$ is obtained by the angle

$$\theta_{i,j} = \begin{cases} \arctan \dfrac{f_{i,j}^{(y)}}{f_{i,j}^{(x)}} & \text{if} \quad f_{i,j}^{(x)} \neq 0 \\ \dfrac{\pi}{2} & \text{if} \quad f_{i,j}^{(x)} = 0, \end{cases} \tag{6.3}$$

   i.e., by the angle between the gradient vector and the x-axis.
3. *Selection of potentially symmetrical pairs of points.* Under the hypothesis that pairs of points having similar gradient directions can not be symmetrical with respect to an axis of symmetry, only the pairs $P_1 = (i_1, j_1)$, $P_2 = (i_2, j_2) \in \mathcal{S}$ for which $|\theta_{i_1,j_1} - \theta_{i_2,j_2}| > \varepsilon_1$ are selected, where ε_1 is a fixed threshold.
4. *Verification of symmetry condition.* For each pair of points $P_1, P_2 \in \mathcal{S}$ selected as described at the previous item, we say that the two points are *symmetrical with respect to an axis of symmetry* if the two gradient vectors form congruent angles with the line joining the two points (see Fig. 7). As a consequence, we define the *condition symmetry* in the following way:

   (i) let $\mathbf{v}_1 = \left(f_{i_1,j_1}^{(x)}, f_{i_1,j_1}^{(y)}\right)$ and $\mathbf{v}_2 = \left(f_{i_2,j_2}^{(x)}, f_{i_2,j_2}^{(y)}\right)$ be the gradient vectors in P_1 and P_2, respectively;
   (ii) let $\mathbf{d}_{12} = (i_2 - i_1, j_2 - j_1)$ and $\mathbf{d}_{21} = (i_1 - i_2, j_1 - j_2)$ be the vectors from P_1 to P_2 and from P_2 to P_1, respectively;
   (iii) let $\alpha_1 = \arccos \dfrac{\mathbf{v}_1 \cdot \mathbf{d}_{12}}{|\mathbf{d}_{12}||\mathbf{v}_1|}$ and $\alpha_2 = \arccos \dfrac{\mathbf{v}_2 \cdot \mathbf{d}_{21}}{|\mathbf{d}_{21}||\mathbf{v}_2|}$ be the angles formed by the gradient vectors $\mathbf{v}_1$ and $\mathbf{v}_2$ with the line passing through P_1 and P_2;
   (iv) we say that P_1 and P_2 are *symmetrical points* if the condition $|\alpha_1 - \alpha_2| < \varepsilon_2$ is verified, where ε_2 is a fixed threshold.

5. *Construction of the midpoint map.* Provided that at the previous item n pairs of points have been identified as symmetrical points, we then define the *midpoint map* as a matrix $M = \{M_{i,j}\}$ of type $I \times J$ with binary values different from 0 just in the n pixels corresponding to the midpoints of each pair.
6. *Hough transform for line detection.* Finally, the application of the Hough transform for lines detection in the midpoint image allows one to detect the axis (or axes) of symmetry.

We provide here some examples.

Example 10 Consider the simple binary image (just two gray levels are allowed) shown at the top of Fig. 8. The computation of the gradient, as previously described, allows the identification of the pixels defining the edge of the

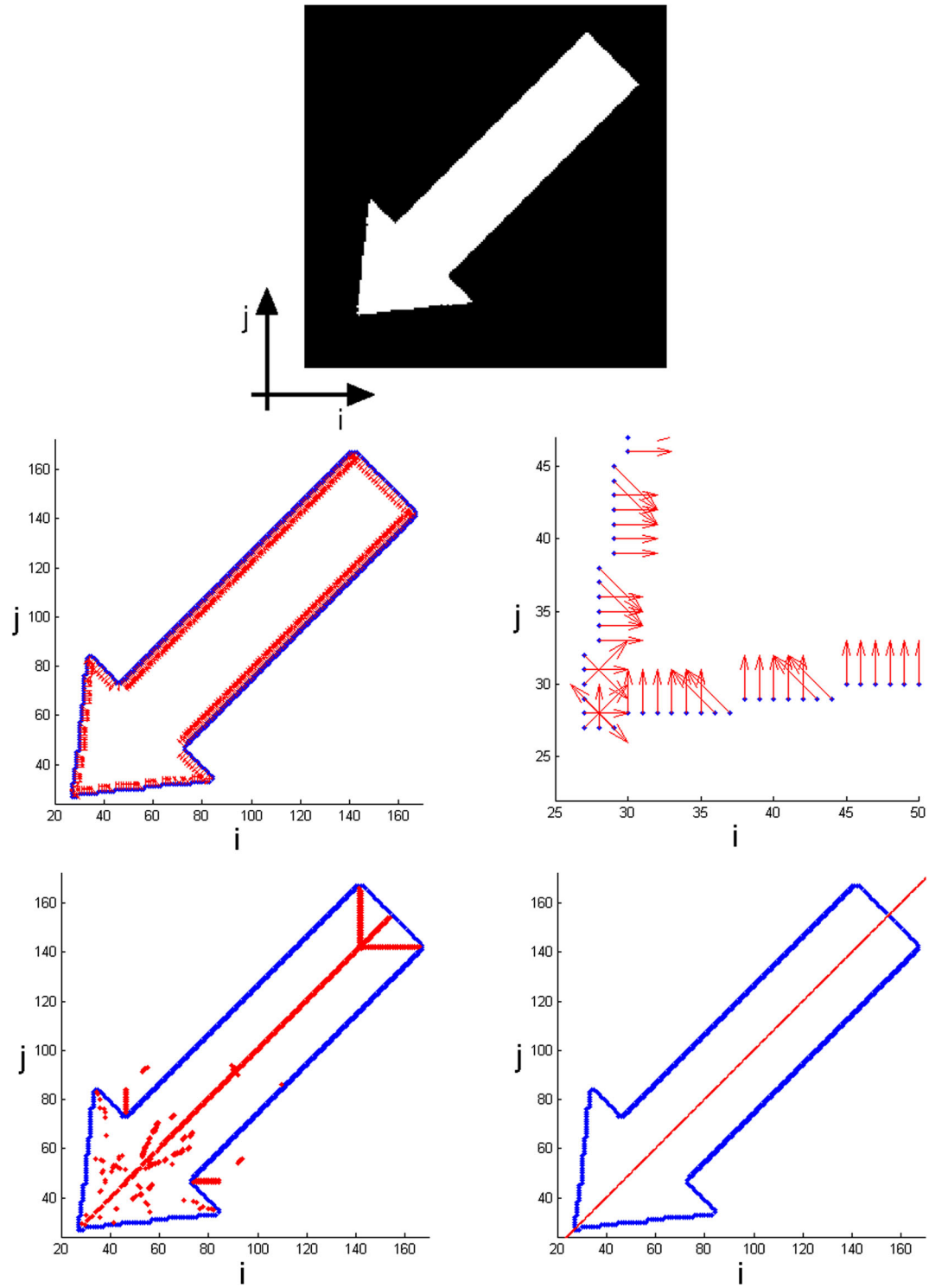

Fig. 8 *Top* original image. *Middle left* edge points (*blue dots*) and gradient vectors (*red arrows*). *Middle right* zoom of the middle left panel. *Bottom left* edge points (*blue dots*) and midpoints (*red dots*). *Bottom right* axis of symmetry (*red line*) identified by applying the Hough transform for line detection to the midpoints set

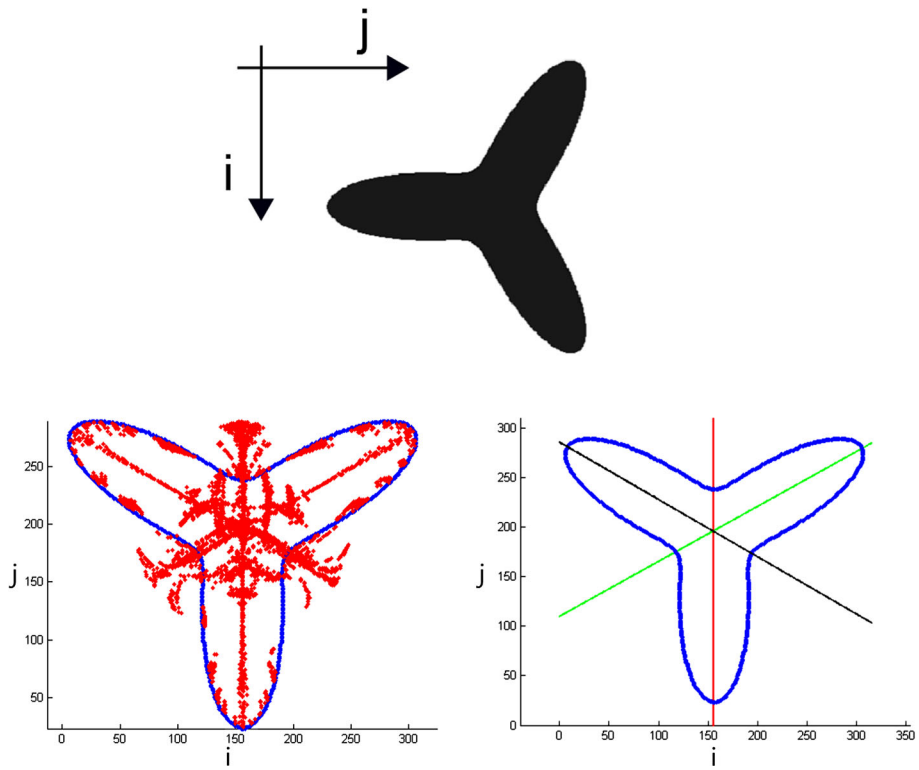

Fig. 9 Detection of the axes of symmetry for the curve with 3 convexities $\mathcal{C}_{a,b}$ with $a = 0.8$, $b = 0.6$. *Top* original image. *Bottom left* edge points (*blue dots*) and midpoints (*red dots*). *Bottom right* edge points (*blue dots*) and the three axes of symmetry

arrow. These pixels can be represented as points in a cartesian plane (blue dots in the middle panels of Fig. 8) where the coordinate axes are related to the row and column indices of the image. The analysis of gradient directions (red arrows in the middle panels of Fig. 8) allows the selection of potentially symmetrical pairs of points, and then the verification of the symmetry condition for building the midpoints map (red dots in the bottom left panel of Fig. 8). As a final step, the application of the Hough transform for line detection to the set of midpoints results in the identification of the axis of symmetry of the arrow shape, as shown in the bottom right panel Fig. 8.

Example 11 The top panel in Fig. 9 represents an image of the region bounded by the graph of the curve with 3 convexities of polar Eq. (4.3),

$$\mathcal{C}_{0.8,0.6} : \rho = \frac{0.8}{1 + 0.6\cos(3\theta)}.$$

The bottom left panel shows the edge points (blue dots) together with the midpoint map (red dots), while the bottom right panel displays the three main axes of symmetry of the curve (red, green and black lines), correctly detected by using the Hough transform for the family of lines expressed in normal parametrization form (3.2).

Example 12 Consider now the region enclosed between two concentric ellipses (see top left panel in Fig. 10) and the corresponding midpoint map we can construct (see top right panel in Fig. 10). Given the intrinsic symmetry of an ellipse, we can meanwhile find a lot of axes of symmetry by iterating the last step of the algorithm (bottom left panel). On the other hand, it could be more interesting to identify a sort of "ellipse-type symmetry" instead of the usual axial symmetry. If we look at the midpoint map we can recognize an ellipse-shape set of midpoints. To identify the equation of a curve best approximating such a shape we can simply follow the argument as in the last step of the algorithm, by using, instead, a family $\mathcal{F} = \{\mathcal{C}_{a,b}\}$ of ellipses $\mathcal{C}_{a,b} : ax^2 + by^2 = 1$ (see bottom right panel).

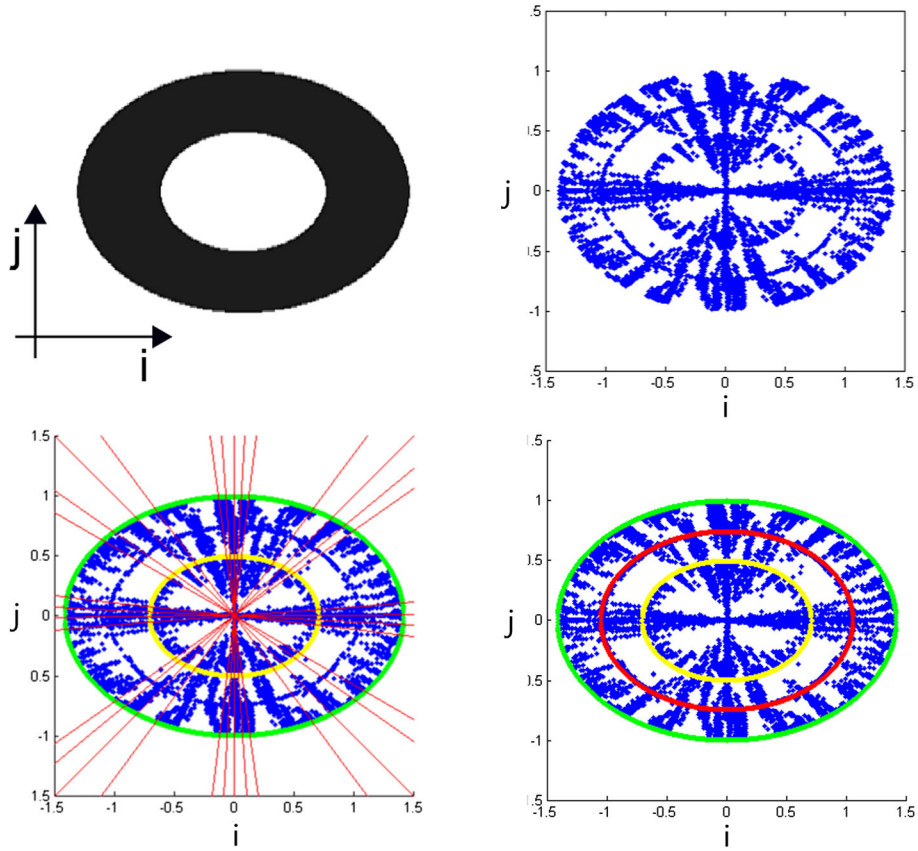

Fig. 10 Detection of symmetries in an image depicting the region enclosed between two ellipses. *Top left* original image. *Top right* the midpoint map. *Bottom left* midpoints (*blue dots*), multiple axes of symmetry (*red lines*) identified by using the Hough transform recognition algorithm and plots of the ellipses used to build the inner and outer profiles of the ring in the original image (equation $\frac{1}{2}x^2+y^2=1$ for the *yellow ellipse*, and $2x^2+4y^2=1$ for the *green* one). *Bottom right* plot of the ellipse of equation $0.9x^2+1.8y^2=1$ (*red line*) identified by applying the Hough transform approach for ellipse detection to the midpoint map

Example 13 Let us now play with elliptic curves, trying to do something similar to what we have done in Example 12. Then, let us consider the image representing a limited portion of the region enclosed between two elliptic curves (see Fig. 11, top left panel) and construct the midpoint map (top right panel) by using the symmetry algorithm. We can now think to a sort of "elliptic-type symmetry" and recognize in the picture an "elliptic-shape" set of midpoints. To identify the equation of a curve best approximating such a shape we can again follow the argument as in the last step of the algorithm, by using, in this case, a family $\mathcal{F}=\{\mathcal{C}_{a,b,m}\}$ of cubic curves expressed in a variant of the Weierstrass form, $\mathcal{C}_{a,b,m}: y^2=mx^3+ax^2+b$ (see the red curve in the bottom panel, Fig. 11).

7 Applications

As outlined in the Sect. 1, the search for symmetries in images is an important issue not only per se, but for several applications in pattern recognition, such as face recognition. The examples provided in the previous section suggest an interesting and innovative way to apply the Hough transform-based technique for symmetry detection, presented in Sect. 6, as a pre-processing step for the Hough transform recognition algorithm, with useful applications, for instance, in medical imaging.

Remark 5.2 highlights the main limitation of the Hough transform recognition procedure: the dimension of the parameter space $\mathbb{A}^t_{(\Lambda_1,\ldots,\Lambda_t)}(\mathbb{R})$ depends on the number t of parameters in the game and, as a consequence, the

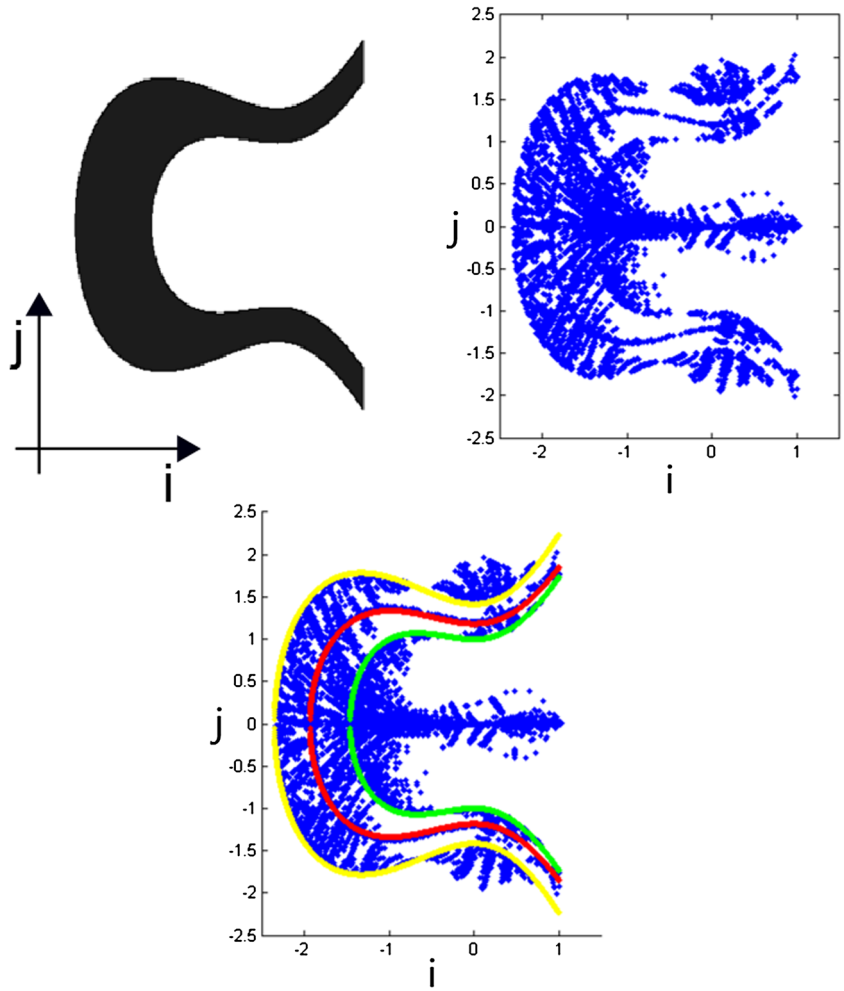

Fig. 11 Detection of symmetries in an image depicting the region enclosed between two elliptic curves. *Top left* original image. *Top right* the midpoint map. *Bottom* plots of the two elliptic curves used to build the two elliptic-shape profiles in the image (equation $y^2 = x^3 + x^2 + 1$ for the *green* elliptic curve, and $y^2 = x^3 + 2x^2 + 2$ for the *yellow* one), and plot of a third elliptic curve of equation $y^2 = 0.81x^3 + 1.2x^2 + 1.4$ (*red line*) identified by applying the Hough transform approach for elliptic curve detection to the midpoint map

complexity of the recognition algorithm exponentially depends on t. Further, increasing the number of parameters has a practical implication, that is, as much as the number t increases as much it becomes difficult to optimally discretize the region $\mathcal{T}$ of the parameter space, where the search for the optimal t-tuple λ^{opt} has to be performed (this potentially reducing the efficiency of the recognition algorithm). On the other hand, in real applications it is mandatory to take into account of possible roto-translations and scaling factors, this leading to the need of finding a good compromise between generality and computational costs. Thus, in practice, one usually restricts to consider families of curves depending on as few parameters as possible, handling heuristically the problem of fixing roto-translations and scaling parameters in a pre-processing step. The question these considerations may raise is:

> How can we proceed to reduce the number t of parameters without loss of generality and without reducing (in fact, possibly increasing) the efficiency of the recognition algorithm?

A possible answer to this question is:

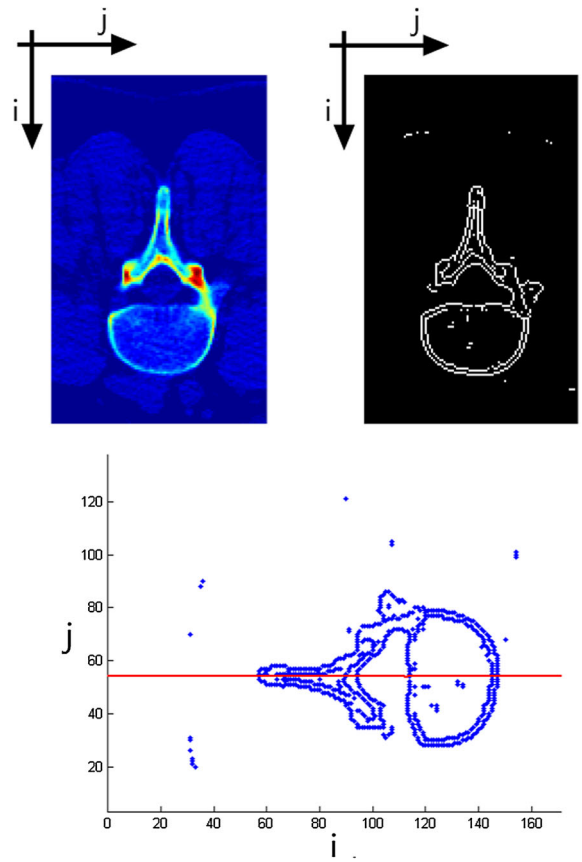

Fig. 12 *Top left* original CT image of a human vertebra. *Top right* binary image containing the edge points obtained by using Sobel operator. *Bottom* axis of symmetry (*red line*) identified by the symmetry algorithm superimposed to the edge points (*blue dots*)

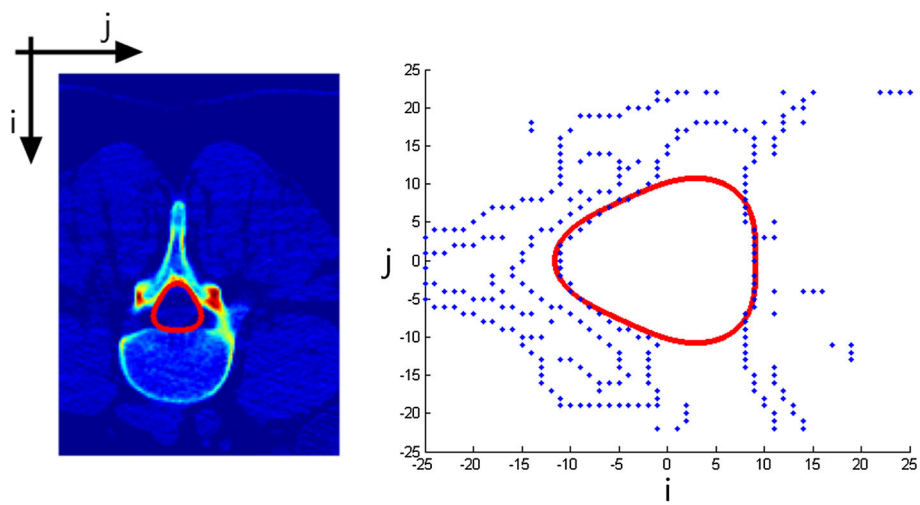

Fig. 13 Recognition of the spinal canal profile of Fig. 12 by using the curve with 3 convexities of Eq. (4.4). *Left* superposition of the recognized curve to the original CT image. *Right* superposition of the recognized curve to the edge points. The curve best approximating the profile turns out to be of equation $(x^2 + y^2)^3 = \left(10.2(x^2 + y^2) - 0.12(x^3 - 3xy^2)\right)^2$

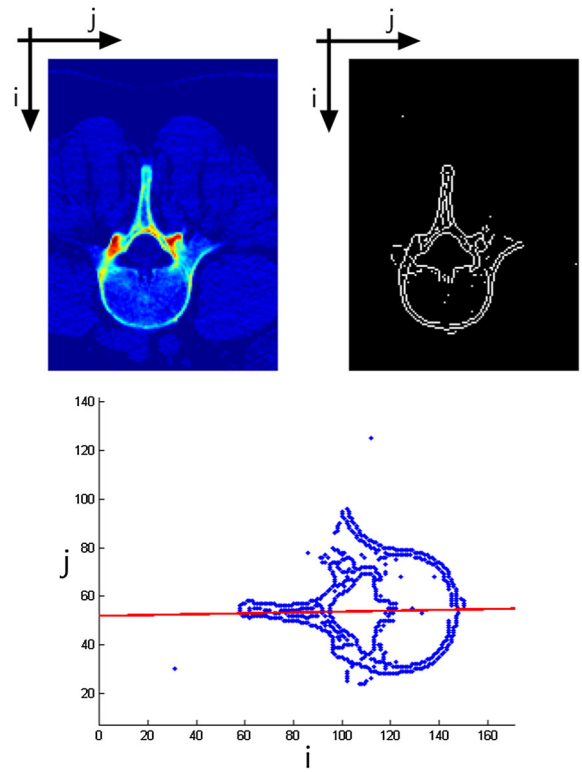

Fig. 14 Example of a vertebra profile not aligned with the coordinate axes. *Top left* original CT image. *Top right* binary image containing the edge points obtained by using Sobel operator. *Bottom* axis of symmetry (*red line*) identified by the symmetry algorithm superimposed to the edge points (*blue dots*)

In order to automatically fix all the parameters concerning roto-translations of the image, we can exploit all information about symmetries we can infer by using the symmetry algorithm described in Sect. 6.

To support this statement, let us recall a problem of great interest in medical imaging: the recognition of bone profiles [6,10,17,18]. As a first example, let us consider a X-ray Computed Tomography (CT) image of a human vertebra (see Fig. 12, top left panel), with the aim to identify the curve best approximating the spinal canal profile. To this end, we will use the family of curves with 3 convexities described in Example 7, in the form of Eq. (4.4), as successfully proposed in [18]. An edge detection algorithm based on the computation of the image gradient allows the extraction of the edge points (see Fig. 12, top right panel) to whom we apply the symmetry algorithm. As shown in the bottom panel of Fig. 12, the axis of symmetry we find is horizontal, suggesting that, in this case, no rotations are needed. Then, the application of the Hough transform recognition algorithm leads to the very good result shown in Fig. 13, where the recognized curve is superimposed to both, the edge points (right panel) and the original image (left panel). Let us now consider a second example where the vertebrae profiles are not perfectly aligned with the axes of the CT acquisition as in Fig. 14, where the application of the symmetry algorithm detects an axis of symmetry with a slope slightly different from zero (Fig. 14, bottom panel). The application of the Hough transform recognition algorithm, without using the information coming from the symmetry algorithm, leads to the non optimal result shown in the top panels of Fig. 15. On the other hand, if we previously rotate the edge points consistently with the slope of the identified axis of symmetry, the Hough transform-based detection technique is able to achieve more precise results in the recognition of the spinal canal profile (see Fig. 15, bottom panels). A different, but analogous, example is presented in Fig. 16.

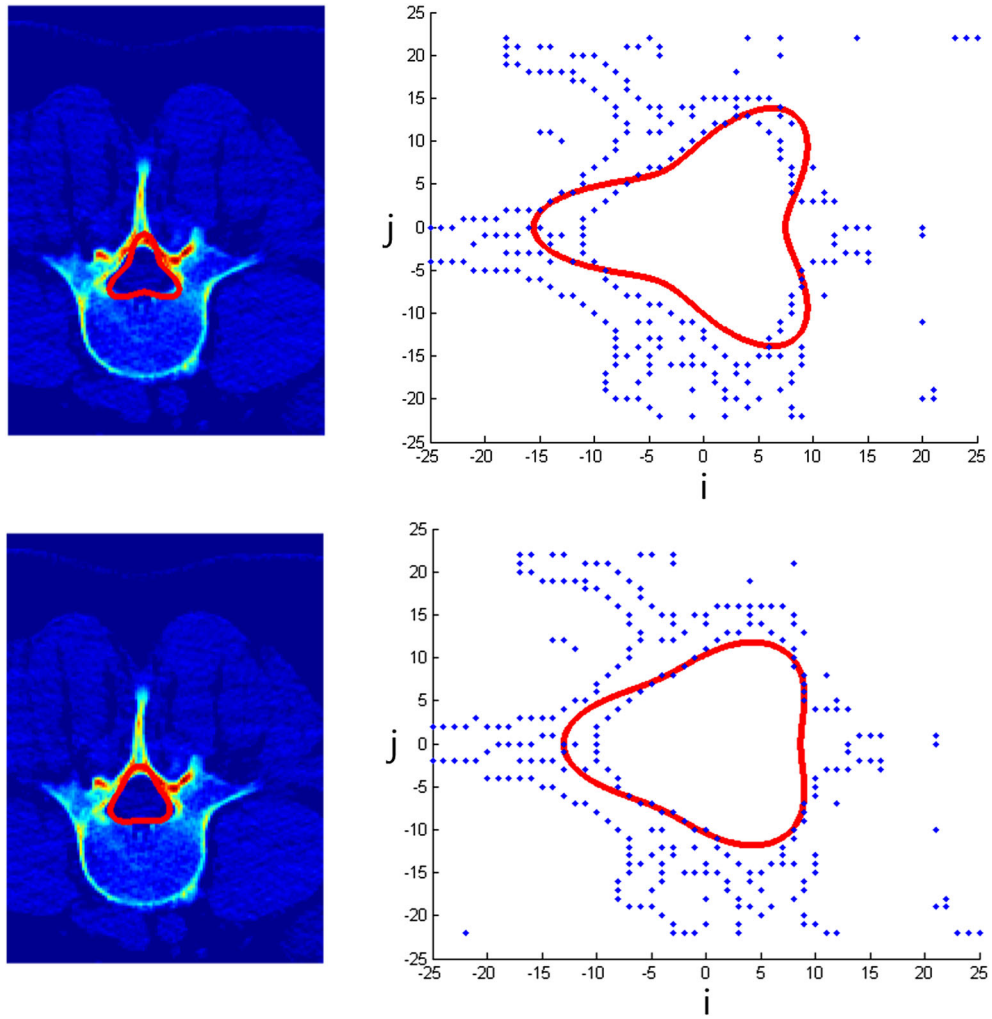

Fig. 15 Recognition of the spinal canal profile in the CT image of Fig. 14 by using the curve with 3 convexities of Eq. (4.4), with or without information on the axis of symmetry. *Top panels* results obtained with no preliminary rotation of the edge points. The recognized curve has equation $(x^2+y^2)^3 = \left(10.1(x^2+y^2) - 0.35(x^3-3xy^2)\right)^2$. *Bottom panels* results obtained with a preliminary rotation of the edge points. The recognized curve has equation $(x^2+y^2)^3 = \left(10.4(x^2+y^2) - 0.2(x^3-3xy^2)\right)^2$

As a final application of the symmetry algorithm, we have considered a stack of 111 CT images of a human spine and, for each slice, we have automatically detected the axis of symmetry of the corresponding vertebra. The algorithm turns out to be very robust with a rate of 72 % cases in which the axis of symmetry has been correctly identified, a rate of 9 % cases where the axis has not been correctly determined, and a remaining 19 % cases in which the detected axis is acceptable but slightly tilted with respect to the true one. In Fig. 17, results corresponding to the processing of six among these 111 slices are presented.

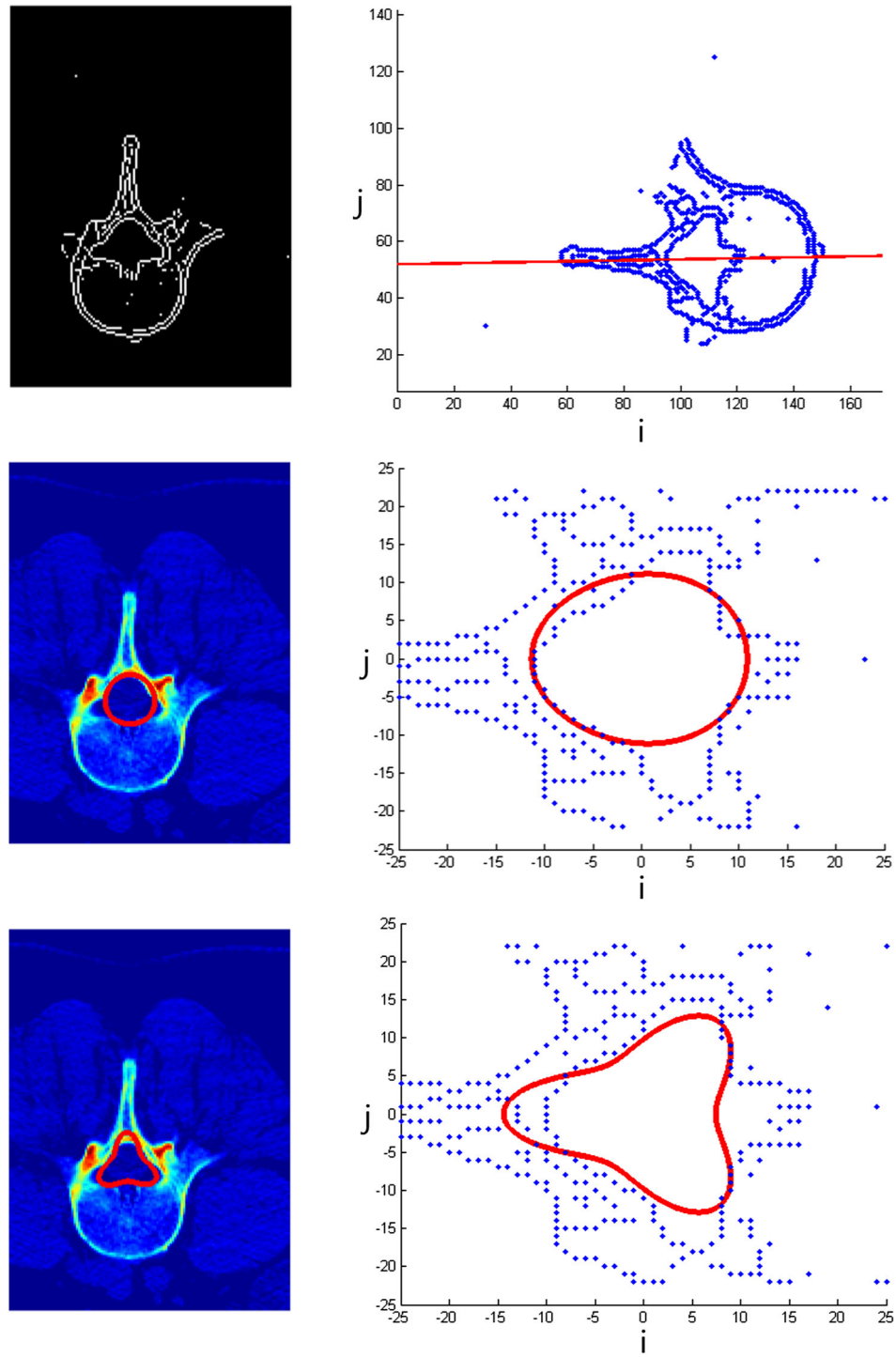

Fig. 16 Recognition of the spinal canal profile in a CT image by using the curve with 3 convexities of Eq. (4.4), with or without information on the axis of symmetry. *Top left* binary image containing the edge points. *Top right* axis of symmetry (*red line*) identified by the symmetry algorithm superimposed to the edge points (*blue dots*). *Middle panels* result obtained with no preliminary rotation of the edge points. The recognized curve has equation $(x^2+y^2)^3 = \left(11.1(x^2+y^2) - 0.02(x^3-3xy^2)\right)^2$. *Bottom panels* result obtained with a preliminary rotation of the edge points. The recognized curve has equation $(x^2+y^2)^3 = \left(9.8(x^2+y^2) - 0.32(x^3-3xy^2)\right)^2$

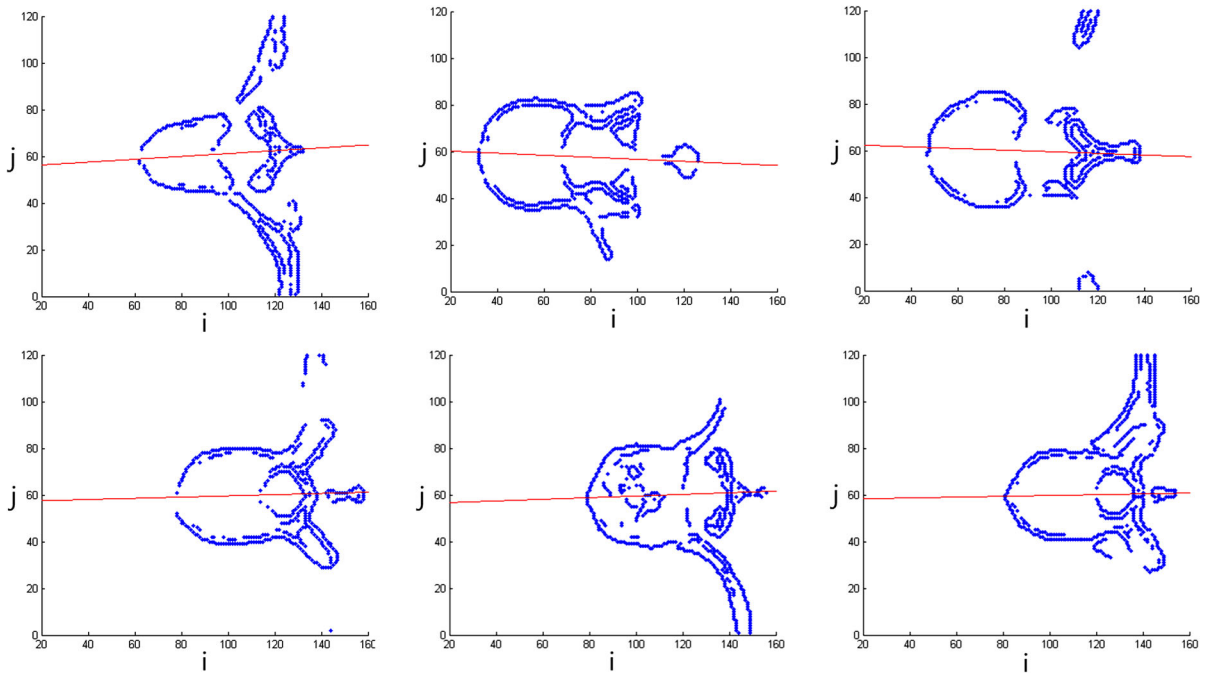

Fig. 17 The symmetry algorithm in action on a whole stack of CT images of a human spine

8 Conclusions

In this paper we develop a Hough-type technique able to identify *curves of symmetry* in images. In the case of straight lines we discuss a real world application in the framework of medical imaging. The general case of various shapes seems to be an intriguing matter in different areas, and it is under investigation. Also, a comparison of our technique with several methods mainly developed in computer vision, quoted in the Sect. 1, appears as a challenging tool for future work.

References

1. Beltrametti, M.C., Carletti, E., Gallarati, D., Monti Bragadin, G.: Lectures on Curves, Surfaces and Projective Varieties—A Classical View of Algebraic Geometry, European Mathematical Society, Textbooks in Mathematics, 9. Translated by F. Sullivan. Zurich (2009)
2. Beltrametti, M.C., Massone, A.M., Piana, M.: Hough transform of special classes of curves. SIAM J. Imaging Sci. **6**(1), 391–412 (2013)
3. Beltrametti, M.C., Robbiano, L.: An algebraic approach to Hough transforms. J. Algebra **371**, 669–681 (2012)
4. Bochnak, J., Coste, M., Roy, M.-F.: Real Algebraic Geometry, Ergeb. Math. Grenzgeb. 36. Springer, Berlin (1998)
5. Cailliere, D., Denis, F., Pele, D., Baskurt, A.: 3D mirror symmetry detection using Hough transform, Image Processing, 2008. ICIP 2008. 15-th IEEE International Conference on Environment and Electrical Engineering, June 10–13, Rome, Italy, pp. 1772–1775 (2015)
6. Campi, C., Perasso, A., Beltrametti, M.C., Massone, A.M.: The Hough transform and a novel prognostic index for chronic leukemia. Preprint (2015)
7. Cham, T.-J., Cipolla, R.: Symmetry detection through local skewed symmetries. Image Vis. Comput. **13**(5), 439–450 (1995)
8. de la Puente, M.J.: Real plane algebraic curves. Expo. Math. **20**(4), 291–314 (2002)
9. Duda, R.O., Hart, P.E.: Use of the Hough transformation to detect lines and curves in pictures. Commun. ACM **15**(1), 11–15 (1972)
10. Fiz, F., Marini, C., Piva, R., Miglino, M., Massollo, M., Bongiovanni, F., Morbelli, S., Bottoni, G., Campi, C., Bacigalupo, A., Bruzzi, P., Frassoni, F., Piana, M., Sambuceti, G.: Adult advanced chronic lymphocytic leukemia: computational analysis of whole-body CT documents a bone structure alteration. Radiology **271**(3), 805–813 (2014)
11. Godement, R.: Cours d'Algèbre, Deuxième Edition, Enseignements de Sciences. Hermann, Paris (1966)
12. Golub, G.H., Van Loan, C.F.: Matrix Computations. 2nd edn. The Johns Hopkins University Press, Baltimore (1989)

13. Gonzalez, R.C., Woods, R.E.: Digital Image Processing. 2nd edn. Prentice Hall, Upper Saddle River (2002)
14. Hassanein, A.S., Mohamed, S., Sameer, M., Ragab, M.E.: A survey on Hough transform, theory, techniques and applications. arXiv:1502.02160v1 [cs.CV] (2015)
15. Hough, P.V.C.: Method and means for recognizing complex patterns, US Patent 3069654, December 18 (1962)
16. Loy, G., Eklundh, J.-O.: Detecting symmetry and symmetric constellations of features. ECCV'06 Proceedings of the 9-th European conference on Computer Vision, Part II, Springer-Verlag, Berlin, Heidelberg, pp. 508–521 (2006)
17. Massone, A.M., Perasso, A., Campi, C., Beltrametti, M.C.: Profile detection in medical and astronomical imaging by means of the Hough transform of special classes of curves. J. Math. Imaging Vis. **51**(2), 296–310 (2015)
18. Perasso, A., Campi, C., Massone, A.M., Beltrametti, M.C.: Spinal canal and spinal marrow segmentation by means of the Hough Transform of special classes of curves. In: Murino V., Puppo E. (eds.) ICIAP 2015, Part I, LNCS,vol. 9279, pp. 590–600 (2015)
19. Princen, J., Illingworth, J., Kittler, J.: A formal definition of the Hough transform: properties and relationships. J. Math. Imaging Vis. **1**, 153–168 (1992)
20. Ricca, G., Beltrametti, M.C., Massone, A.M.: An iterative approach to Hough transform without re-voting. arXiv:1407.3969v1 [cs.CV] (2014)
21. Ricca, G., Beltrametti, M.C., Massone, A.M.: Piecewise recognition of bone skeleton profiles via an iterative Hough transform approach without re-voting. Proc. SPIE 9413, Medical Imaging 2015: Image Processing, vol. 9413, p. 94132M (2015)
22. Robbiano, L.: Hyperplane sections, Gröbner bases, and Hough transforms. J. Pure Appl. Algebra **219**, 2434–2448 (2015)
23. Sendra, J.R., Winkler, F., Pérez-Diaz, S.: Rational Algebraic Curves—A Computer Algebra Approach, Algorithms and Computation in Mathematics, vol. 22. Springer, Berlin (2008)
24. Shikin, E.V.: Handbook and Atlas of Curves. CRC Press, Inc., Boca Raton (1995)
25. Torrente, M.-L., Beltrametti, M.C.: Almost-vanishing polynomials and an application to the Hough transform. J. Algebra Appl. **13**(8), 1450057 (39 pp.) (2014)
26. Yip, R.K.K.: A Hough transform technique for the detection of parallel projected rotational symmetry. Pattern Recognit. Lett. **20**, 991–1004 (1999)
27. Yuen, K.S.Y., Chan, W.W.: Two methods for detecting symmetries. Pattern Recognit. Lett. **15**(3), 279–286 (1994)